
Electronic Thesis and Dissertation Repository

8-6-2020 10:00 AM

The Role of Regulator of G Protein Signaling 2 in Inflammatory Cytokine Release in Endotoxemia in Mice

Xin Tong Ma, *The University of Western Ontario*

Supervisor: Feng, Qingping, *The University of Western Ontario*

Co-Supervisor: Chidiac, Peter, *The University of Western Ontario*

A thesis submitted in partial fulfillment of the requirements for the Master of Science degree in Physiology and Pharmacology

© Xin Tong Ma 2020

Follow this and additional works at: <https://ir.lib.uwo.ca/etd>



Part of the [Cardiovascular Diseases Commons](#), [Cellular and Molecular Physiology Commons](#), and the [Immune System Diseases Commons](#)

Recommended Citation

Ma, Xin Tong, "The Role of Regulator of G Protein Signaling 2 in Inflammatory Cytokine Release in Endotoxemia in Mice" (2020). *Electronic Thesis and Dissertation Repository*. 7317.
<https://ir.lib.uwo.ca/etd/7317>

This Dissertation/Thesis is brought to you for free and open access by Scholarship@Western. It has been accepted for inclusion in Electronic Thesis and Dissertation Repository by an authorized administrator of Scholarship@Western. For more information, please contact wlsadmin@uwo.ca.

Abstract

In sepsis, lipopolysaccharide (LPS) activates toll-like receptor 4 to stimulate the release of inflammatory cytokines (*e.g.* tumor necrosis factor- α , TNF- α), leading to cardiac dysfunction. Regulator of G protein signaling 2 (RGS2) limits G protein-coupled receptor signaling by increasing the rate of G protein deactivation or inhibiting G protein-effector interactions. We hypothesized that RGS2 deficiency would enhance proinflammatory responses in endotoxemia. Adult wild-type and *RGS2*^{-/-} C57BL/6 mice and neonatal cardiomyocytes were treated with LPS and assessed for inflammatory responses and cardiac function. Myocardial TNF- α expression was higher in *RGS2*^{-/-} mice during endotoxemia. Additionally, cardiac function was impaired in *RGS2*^{-/-} mice. Phosphorylated p38 levels were higher in the *RGS2*^{-/-} myocardium in endotoxemia. *In vitro*, TNF-expression was higher in *RGS2*^{-/-} cardiomyocytes after LPS stimulation. Our study suggests that RGS2 is cardioprotective and inhibits proinflammatory signaling via p38 in sepsis. Thus, this study suggests a novel therapeutic target for the clinical treatment of sepsis.

Keywords

sepsis, regulator of G protein signaling 2 (RGS2), cardiac dysfunction, endotoxemia, TNF- α , inflammatory cytokine release

Summary for Lay Audience

Sepsis is a major cause of death globally and of in-hospital mortality in Canada. It is caused by an improper response to infection, resulting in inflammation and organ failure. However, there are no drugs specifically targeted for sepsis. The bacterial component, lipopolysaccharide (LPS), causes sepsis by stimulating a proinflammatory response, leading to heart dysfunction and patient death. G protein-coupled receptors (GPCRs) are a family of receptors found in many tissues that regulate a variety of cellular processes. GPCR activities can be limited by regulator of G protein signaling 2 (RGS2). While both RGS2 regulated GPCR signaling and LPS induced inflammatory pathway are well established, how the two signaling pathways interact is not known. The aim of this thesis was to determine the role of RGS2 in LPS induced inflammation in the heart, and identify factors modulated by RGS2. Adult wild-type and RGS2 deficient mice were challenged with LPS, while newborn mouse cardiac cells were isolated and treated with LPS. They were then assessed for inflammatory responses by measuring the levels of TNF- α , a proinflammatory factor. Results show that TNF- α expression was induced by LPS in wild-type mice, and the response was further enhanced in the heart of RGS2 deficient mice. Similarly, LPS-induced TNF- α expression was higher in RGS2 deficient cardiomyocytes. Furthermore, LPS-induced activity of p38, an inflammatory mediator, was also higher in the heart of RGS2 deficient mice. Notably, heart dysfunction was worse in RGS2 deficient mice in sepsis. In conclusion, RGS2 is protective and can inhibit the proinflammatory response in sepsis. This thesis may open up new strategies in the design of drugs for the treatment of sepsis.

Co-Authorship Statement

Dr. Qingping Feng and Dr. Peter Chidiac supervised and guided the design of all experiments. Xiangru Lu provided training and assistance overall with experimental methods and data collection and analysis.

Acknowledgments

First and foremost, I'd like to express my deepest gratitude to my supervisors, Dr. Qingping Feng and Dr. Peter Chidiac. This thesis would not have been possible without their guidance and support. They have taught me to become a better scientist and provided a fulfilling graduate experience that fostered learning and critical thinking. I am grateful for the invaluable skills I developed under their mentorship and look forward to applying it in my future career. I would also like to thank my research advisory committee, Dr. Douglas Jones and Dr. Wei-Yang Lu, who provided brilliant insight and encouragement with endless patience. I am blessed to have a team of incredibly knowledgeable advisors to impart their wisdom and inspire me.

I would like to thank all the lab members who helped me throughout my Masters and made it an enjoyable experience. A huge thank you to Dr. Xiangru (Sharon) Lu for her guidance and sharing her knowledge and experience. Thank you for teaching me all the technical skills required in the lab, from animal work and molecular techniques to data analysis. She is the rock of the Feng lab, and I am very fortunate to have her advise me both inside and outside of lab. Thank you to Dr. Anish Engineer and Elizabeth Greco for your guidance and friendship. There was never a dull moment in the lab, and I will cherish our many discussions and experiences shared. I am thankful for Xiaoyan Wang, Matthew Novello, Fang Ye, and Gregory Robinson for their constant support. Thank you to Brent Tschirhart for providing a colourful environment in the lab and your never-ending repertoire of stories. Thank you to my friends and 4th year students in the Phys/Pharm department for all the camaraderie and good times.

Finally, thank you to my friends for their continuous support and believing in me. Even spread across the continent, you never failed to constantly encourage and cheer me on. I am also very grateful for my family. Thank you to my parents, who are my inspiration and have shown me the importance of education and perseverance. Their trust and love for me have shone through my darkest days. Thank you to my grandparents and extended family, whose support can be felt even across the world.

Table of Contents

Abstract.....	i
Summary for Lay Audience.....	ii
Co-Authorship Statement.....	iii
Acknowledgments.....	iv
Table of Contents.....	v
List of Tables.....	viii
List of Figures.....	ix
List of Appendices.....	xi
List of Abbreviations.....	xii
Chapter 1.....	1
1 Introduction.....	1
1.1 Sepsis.....	1
1.1.1 Endotoxemia as a model of sepsis.....	2
1.2 Sepsis-induced cardiac dysfunction.....	3
1.2.1 Proinflammatory cytokine and cardiac dysfunction.....	3
1.2.2 Cardiomyocytes in sepsis.....	4
1.3 Toll-like receptors (TLRs).....	5
1.3.1 Toll-like receptor 4 (TLR4).....	5
1.4 Mitogen-activated protein kinases in sepsis.....	8
1.5 NF- κ B in inflammatory signaling.....	9
1.6 G protein-coupled receptors.....	10
1.6.1 G-protein signaling regulates MAPK activity.....	12
1.6.2 G protein signaling in sepsis.....	13
1.7 Regulators of G protein signaling.....	15

1.7.1	Regulator of G protein signaling 2.....	17
1.8	Summary and rationale	18
1.9	Hypothesis and aims	21
Chapter 2	23
2	Materials and Methods.....	23
2.1	<i>In vivo</i> C57BL/6 mouse model	23
2.1.1	LPS-induced endotoxemia mouse model.....	23
2.2	Primary neonatal cardiomyocyte cell culture	23
2.2.1	Isolation of neonatal cardiomyocytes	23
2.2.2	LPS-induced inflammatory cytokine release in cardiomyocytes.....	24
2.2.3	PKA inhibition in LPS-induced inflammatory cytokine release	24
2.2.4	Immunohistochemistry of cardiomyocytes.....	25
2.3	Quantitative polymerase chain reaction.....	26
2.3.1	RNA isolation from LV tissues.....	26
2.3.2	RNA isolation from cardiomyocytes	27
2.3.3	Reverse transcription	27
2.3.4	Quantitative real-time PCR.....	27
2.4	TNF- α ELISA	28
2.5	NF- κ B activity	28
2.5.1	Nuclear protein extraction.....	28
2.5.2	NF- κ B ELISA.....	29
2.6	Western Blotting	29
2.6.1	Protein lysis from LV tissues.....	29
2.6.2	Protein lysis from cardiomyocytes.....	30
2.6.3	Immunoblotting.....	30
2.7	Echocardiography	32

2.8 Statistical analysis.....	33
Chapter 3.....	34
3 Results.....	34
3.1 Body weight and litter size	34
3.2 RGS2 mRNA levels in the heart during endotoxemia.....	35
3.3 TNF- α mRNA and protein levels in the heart after LPS treatment <i>in vivo</i>	37
3.4 TNF- α mRNA and protein levels in cardiomyocytes	40
3.5 Interleukin mRNA levels in the heart during endotoxemia	42
3.6 Left ventricular cardiac function in endotoxemia.....	45
3.7 MAPK phosphorylation levels in the heart.....	49
3.8 PKA-inhibition in cardiomyocytes	52
3.9 Relative NF- κ B activity in the heart.....	54
Chapter 4.....	56
4 Discussion	56
4.1 Summary	56
4.2 RGS2 deficiency affects body weight and litter size	56
4.3 RGS2 deficiency enhances the TNF- α proinflammatory response during endotoxemia.....	57
4.4 Interleukin release is not affected by RGS2 deficiency	59
4.5 Cardiac dysfunction is exacerbated in <i>RGS2</i> deficient mice	59
4.6 p38 may be involved in a crosstalk mechanism.....	60
4.7 Limitations and future directions	62
4.8 Conclusions.....	63
References.....	65
Appendices.....	85
Curriculum Vitae	87

List of Tables

Table 2.1. Forward and reverse primer sequences and specific annealing temperature for genes of interest	28
Table 2.2. Primary antibody concentrations and the corresponding secondary antibody concentrations used for immunoblotting.	31
Table 3.1. Tabular summary of cardiac function in WT and <i>RGS2</i> ^{-/-} mice analyzed by short-axis M-mode echocardiography.....	48

List of Figures

Figure 1.1. LPS stimulation of TLR4 leads to proinflammatory cytokine release	7
Figure 1.2. Conventional signaling pathways of G α s and G α q activity	11
Figure 1.3. RGS2 regulation of G protein signaling	16
Figure 1.4. Possible crosstalk mechanisms involving the role of RGS2 in limiting G protein signaling activity	20
Figure 2.1: Efficacy of the isolation of neonatal cardiomyocytes	26
Figure 3.1. Body weight (g) of WT and <i>RGS2</i> ^{-/-} mice	34
Figure 3.2: Litter sizes of WT and <i>RGS2</i> ^{-/-} mice	35
Figure 3.3. RGS2 mRNA level in WT LV after LPS treatment <i>in vivo</i>	36
Figure 3.4. WT and <i>RGS2</i> ^{-/-} LV TNF- α mRNA levels 2 hours after LPS treatment	38
Figure 3.5. Plasma TNF- α levels in WT and <i>RGS2</i> ^{-/-} during endotoxemia	39
Figure 3.6. LPS-induced TNF- α levels in WT and <i>RGS2</i> ^{-/-} cardiomyocytes	41
Figure 3.7. Myocardial IL-6 mRNA levels in WT and <i>RGS2</i> ^{-/-} mice after LPS treatment <i>in vivo</i>	43
Figure 3.8. Myocardial IL-1 β mRNA levels in WT and <i>RGS2</i> ^{-/-} mice after LPS treatment <i>in vivo</i>	44
Figure 3.9. Representative short-axis and M-mode images of the left ventricle in WT and <i>RGS2</i> ^{-/-} mice	46
Figure 3.10. LV ejection fraction and fractional shortening in WT and <i>RGS2</i> ^{-/-} mice	47
Figure 3.13. Myocardial ERK1/2 phosphorylation after LPS treatment <i>in vivo</i>	50
Figure 3.12. Myocardial p38 MAPK phosphorylation after LPS treatment <i>in vivo</i>	51

Figure 3.13. TNF- α mRNA levels in WT and *RGS2*^{-/-} cardiomyocytes after PKA inhibition 53

Figure 3.14. Relative NF- κ B activity in WT and *RGS2*^{-/-} myocardium during endotoxemia 55

Figure 4.1: Schematic of RGS2 regulation of TNF- α expression during endotoxemia in the heart..... 64

List of Appendices

Appendix A: Animal use protocol approved by the Animal Care Committee	85
---	----

List of Abbreviations

CARS	compensatory anti-inflammatory response syndrome
DMSO	dimethyl sulfoxide
DTT	dithiothreitol
EDTA	ethylenediaminetetraacetic acid
ELISA	enzyme-linked immunosorbent assay
GAP	GTPase activating protein
GDP	guanine diphosphate
GPCR	G protein-coupled receptor
GTP	guanine triphosphate
IL	interleukin
IP	intraperitoneal
IP ₃	inositol 1,4,5-trisphosphate
LPS	lipopolysaccharide
LV	left ventricle
MAPK	mitogen-activated protein kinase
NF- κ B	nuclear factor kappa-light-chain-enhancer of activated B cells
P	postnatal day
PAMP	pathogen associated molecular pattern
PBS	phosphate buffered saline

PKA	protein kinase A
PKC	protein kinase C
PLC	phospholipase C
qPCR	quantitative polymerase chain reaction
RGS	regulator of G protein signaling
SIRS	systemic inflammatory response syndrome
TBS-T	tris-buffered saline with 0.1 % Tween 20
TLR	toll-like receptor
TNF- α	tumor necrosis factor α
WT	wild-type

Chapter 1

1 Introduction

1.1 Sepsis

Sepsis is a life-threatening condition caused by a dysregulated host response to infection.¹ It is a leading cause of death due to infection globally and occurs in 2-11% of patients in hospitals and intensive care units.^{2,3} Currently, one in five deaths worldwide is due to sepsis.⁴ While there has been a decreasing trend in sepsis burden globally from 1990-2017, an estimate of 11 million sepsis-related deaths were reported for 2017.⁴ Among these cases, males had higher mortality than females.⁴ The population at risk include young children as well as adults 65 years and older, which is a cause for concern with the global aging population.^{4,5} Sepsis cases and mortality rates are different depending on location, with the highest impact on countries with low socio-demographic index, which is an indicator of socio-demographic development.⁴ Countries such as sub-Saharan Africa, Oceania, south Asia, east Asia, and southeast Asia had the highest burden in 2017, which may be due to lack of access to supportive treatments.⁴ Survivors of sepsis often experience long term consequences that decrease their quality of life.⁶⁻⁸ Sepsis is independently associated with increased risk of cognitive impairment and functional limitations, which correlates with increased healthcare needs, depression, and mortality.⁸ Thus, in addition to implications for patients and their families, sepsis has a major impact on the healthcare system.

Severe cases of sepsis may lead to multi-organ failure and septic shock.^{1,9} In North America and Europe, approximately 7% of admitted intensive care unit patients have septic shock.¹⁰ Septic shock is defined as a subset of sepsis, in which circulatory and metabolic abnormalities increase mortality. According to the most recent Sepsis-3 definition, clinical criteria for septic shock include the presence of both hypotension and hyperlactemia.¹ Specifically, septic shock patients are identified as having enduring hypotension that requires vasopressors to sustain mean arterial pressure (MAP) above 65 mmHg, and a serum lactate level above 2 mmol/L (18 mg/dL) despite volume resuscitation treatment.^{1,11} The first-line vasopressor used for septic shock is norepinephrine, and it is recommended

to be used alongside fluid resuscitation to attain the target MAP \geq 65 mmHg.¹² The presence of both hypotension and hyperlactemia broadly encompasses cardiovascular and cellular impairment and is correlated with significantly higher mortality. In North America and Europe, septic shock has a mortality rate of about 38%. Globally, hospital mortality for such patients is above 40%.^{1,10}

Sources of infection that may lead to sepsis include bacterial, fungal, viral, and parasitic pathogens.⁴ While an appropriate immune response is necessary to combat and clear infections to protect the host, an improper immune response can be harmful to the host. This aberrant immune response has two phases. In the initial stage of sepsis, patients often show a drastic increase in proinflammatory response as characterized in systemic inflammatory response syndrome (SIRS). As sepsis progresses, patients enter an immunosuppressive state, characterizing the compensatory anti-inflammatory response syndrome (CARS).¹³ The excessive inflammation found in the SIRS causes collateral tissue and organ damage, while the CARS stage is thought to be responsible for increasing patient susceptibility to secondary infections.¹⁴ While sepsis is described as two stages, it is more complex in humans as both phases follow a variable time course and do not always appear at separate times. Due to the heterogeneity of sepsis, this makes it difficult to study in humans.

In the past two decades, studies have reported higher survival rates which have been attributed to improvements in supportive therapies for septic shock patients.^{15,16} Currently, there are no approved targeted therapeutics to directly combat sepsis. Rather, treatments such as antibiotics and fluid resuscitation are focused on the cause of the infection and life support measures, respectively.^{15,17}

1.1.1 Endotoxemia as a model of sepsis

The pathogenesis of sepsis is caused by a pathogen that can trigger a systemic inflammatory response – 50% of which are of microbial origin.¹⁸ Of these, gram-positive and gram-negative bacteria are responsible for approximately 50% and 40% of infections respectively.³ Endotoxin/lipopolysaccharide (LPS) found on the gram-negative bacteria contributes to sepsis pathogenesis through a well-defined intracellular signaling cascade.¹⁹

It activates downstream pathways of toll-like receptor 4 (TLR4) to stimulate the release of proinflammatory cytokines. Murine endotoxemia models have been used for almost 100 years to simulate sepsis in humans.²⁰ While it does not fully recapitulate septic conditions in humans, endotoxemia is a scientifically useful model for investigating specific pathways and mechanisms during septic immune responses.²⁰

1.2 Sepsis-induced cardiac dysfunction

Globally, close to half of all sepsis-related deaths occur due to an underlying injury or non-communicable disease with sepsis complications.⁴ Organ dysfunction in sepsis most commonly compromises the respiratory and cardiovascular systems. Cardiovascular effects primarily result in an elevated serum lactate level or hypotension. SIRS may contribute to persistently elevated lactate levels post cardiac arrest.¹¹ Additionally, patients with cardiogenic shock after heart surgery may have increased lactate levels due to elevated lactate production.²¹ Serum lactate level is an important indicator in predicting mortality in cardiogenic shock patients treated with extracorporeal membrane oxygenation.²² Similarly, hypotension persists as sepsis progresses, and myocardial dysfunction may occur.¹⁴ Myocardial dysfunction is a common complication of septic shock and a major predictor of mortality in sepsis, and occurs in 40% of sepsis patients.²³⁻²⁵ The mortality rate of these patients can be as high as 70%.²³⁻²⁵

The pathophysiology of sepsis-induced cardiac dysfunction is suggested to be functional, and not due to physical structural changes. Previous studies showed that dysfunction may be reversible in 7-10 days.²⁶ There are two phases of septic shock that are characterized by different parameters of myocardial dysfunction. The early “warm” phase is hyperdynamic shock. It is comprised of high cardiac output, low peripheral vascular resistance, and increased temperature in the extremities of the body. This is followed by the late “cold” phase of hypodynamic shock, which is indicated by hypotension, low cardiac output, poor peripheral perfusion, and cold extremities. The latter phase may be followed by death.^{27,28}

1.2.1 Proinflammatory cytokine and cardiac dysfunction

The detrimental effect of LPS on cardiac function is mediated through the production of proinflammatory cytokines.²⁹ LPS-stimulated proinflammatory cytokines, particularly

tumor necrosis factor (TNF)- α and interleukin 6 (IL-6), have been suggested to be main components in cardiac dysfunction.²⁵ Patients with sepsis often have impaired cardiac function as a consequence of elevated proinflammatory cytokine levels.³⁰ As well, the LPS-activated TLR4 pathway has a direct role in cardiac dysfunction in sepsis. Previous studies showed that TLR4 knockout mice have reduced cardiac depression and lower myocardial proinflammatory cytokine expression when challenged with LPS injection compared to wild-type mice.³¹ This suggests that LPS binding to TLR4 in cardiomyocytes resulting in downstream activation of NF- κ B and proinflammatory cytokine release during endotoxemia regulates cardiac depression.

Similarly, TNF- α administration has been shown to induce symptoms similar to sepsis with multi-organ failure, including hypotension, pulmonary and gastrointestinal hemorrhage, tubular necrosis and death.³² High levels of TNF- α produced in the myocardium contribute to the development of cardiac dysfunction.³³ The high cytokine levels depress cardiac contractile function in live animals and isolated cardiomyocytes.^{34,35} LPS-induced myocardial dysfunction is abrogated by treatment with TNF- α antiserum, and administration of TNF- α binding proteins preserve myocardial function in mice in endotoxemia.^{33,34} Thus, TNF- α activity plays an important role in LPS-induced myocardial dysfunction.

1.2.2 Cardiomyocytes in sepsis

Cardiomyocytes account for about 70% of the mammalian heart mass.³⁶ The severity of sepsis-induced cardiac dysfunction is a prognostic factor of sepsis. As such, one strategy in combating sepsis is the prevention of cardiomyocyte damage.

Previous studies showed that cardiomyocytes produce and secrete proinflammatory cytokines after LPS treatment in both mice and humans.^{33,37} As well, LPS binding to TLR4 induced inflammation in stem-cell derived cardiomyocytes *in vitro*.³⁷ In HL-1 cardiac muscle cells, troponin I expression was enhanced when treated with LPS.³⁸ Additionally, LPS stimulation resulted in higher troponin levels in both HL-1 and human cardiomyocyte supernatant.³⁸ Troponin I is a marker of myocardial injury and may indicate myocardial involvement in sepsis.²⁴ Elevated levels of cardiac troponin I are detected in patients with

severe sepsis and septic shock.³⁹ Furthermore, release of cardiac troponin I during sepsis is a predictor of mortality in septic patients, and may be dependent on cytokine levels or caused by myocardial membrane leakage.^{40,41} Thus, cardiomyocytes are involved in sepsis pathogenesis.

1.3 Toll-like receptors (TLRs)

Toll-like receptors (TLRs) are a family of protein receptors that can recognize a variety of pathogen associated molecular patterns (PAMPs). As such, they are important for innate immune responses. TLRs dimerize and are activated by PAMPs, resulting in downstream signaling to initiate innate immune response.⁴² All TLRs share a conserved N-terminal extracellular region composed of leucine-rich-repeat (LRR) domains and a C-terminal cytoplasmic region.⁴² The LRR domains are essential for pathogen recognition through protein-protein interactions.⁴³ In humans, TLR1-10 are found, and among these TLR2, TLR3, TLR4, TLR5, and TLR9 have been shown to be involved in recognizing microbial pathogens.⁴⁴ Of interest to the present study, TLR4 mainly recognizes LPS and has a role in the release of proinflammatory cytokines, which may lead to sepsis.⁴⁵

1.3.1 Toll-like receptor 4 (TLR4)

TLR4 is primarily found in cells of myeloid origin (*e.g.* macrophages, dendritic cells), but it is also expressed in cardiomyocytes and endothelial cells.⁴⁶⁻⁴⁸ TLR4 signaling has a central role in the innate immune response. LPS activates TLR4 to stimulate inflammatory cytokine release and innate immune responses, which is the immediate host defense against microbial pathogens.⁴⁹ Thus, TLR4 signaling pathway has an important role in the pathogenesis of sepsis.

LPS does not directly bind to TLR4. Rather, it binds to LPS-binding protein (LBP), which is a phospholipid transport protein that facilitates LPS binding to cluster of differentiation 14 (CD-14), a membrane glycoprotein.⁴⁹ With the additional interaction with lymphocyte antigen 96, also known as MD-2, which recognizes and binds the lipophilic domain of LPS (lipid A), this complex promotes TLR4 to dimerize and induce downstream signaling. Activated TLR4 can either recruit myeloid differentiation factor (MyD) 88 or become internalized into endosomes and interact with TIR-domain-containing adapter-inducing

interferon- β (TRIF). Both pathways are mutually exclusive.⁵⁰ The MyD88-dependent pathway results in the activation of nuclear factor kappa-light-chain-enhancer of activated B cells (NF- κ B) and production of proinflammatory cytokines, such as IL-6, IL-1 β , and TNF- α , whereas the TRIF-dependent pathway results in the slower activation of NF- κ B and the transcription of the interferon (IFN)- β gene.^{49,51}

The association of MyD88 to TLR4 further recruits interleukin-1 receptor-associated protein kinases (IRAKs). This triggers downstream signaling pathways including Rac1 and NADPH oxidase. Additionally, recruited IRAKs activate downstream TNFR-associated factor 6 (TRAF6), leading to the subsequent activation of transforming growth factor- β -activated kinase 1 (TAK1). This leads to the activation of transcription factors such as NF- κ B and the production of proinflammatory cytokines.¹⁹ As well, a parallel downstream pathway of MyD88 is the simultaneous activation of mitogen-activated protein kinases (MAPKs), which leads to further activation of inflammatory cytokines (Figure 1.1).⁵²

Activation of TLR4 by LPS result in the release of inflammatory cytokines, and TNF- α is released within 30–90 min after LPS stimulation.⁵³ Subsequently, activation of inflammatory cascades and upregulation of adhesion molecules result in inflammatory cell migration into tissues.⁵³ Additionally, excessive release of proinflammatory mediators stimulate the production of reactive oxygen species and nitric oxide, resulting in tissue damage and inducing further inflammatory response.⁵⁴ Damaged tissues will produce endogenous damage-associated molecular patterns (DAMPs), which will activate TLRs and exacerbate the immune response. Finally, this inflammatory cycle may cause organ failure, cardiac dysfunction, and eventually death.²⁷ Inhibition of TLR4 was shown to alleviate the detrimental effects of LPS.⁵⁵ Similarly, blocking LPS-TLR4 association is protective against endotoxic shock in humans.⁵⁶ In clinical settings, modeling TLR4 expression allowed an accurate characterization of the clinical outcomes of sepsis patients.⁵⁷ Thus, overactivation of TLR4 by LPS contributes to the pathogenesis of sepsis.

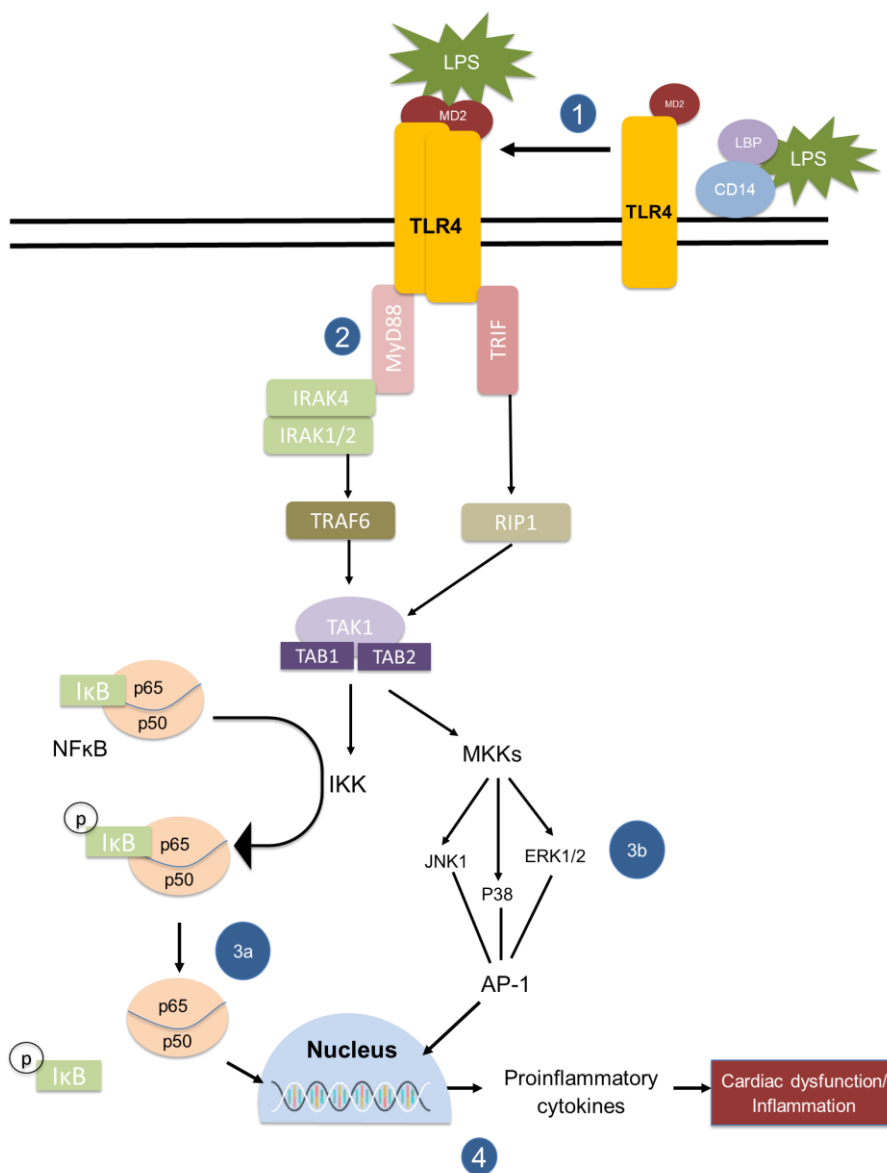


Figure 1.1. LPS stimulation of TLR4 leads to proinflammatory cytokine release. 1. LPS interacts with LBP, which facilitates binding to glycoprotein CD14. This binding structure interacts with MD-2 to bind to TLR4. TLR4 dimerizes upon LPS activation of the receptor. 2. TLR4 activation recruits MyD88. This interaction further recruits IRAK1 and IRAK6. This complex activates further downstream signaling pathways. 3a. NF- κ B is activated following I κ B phosphorylation. 3b. MAPKs JNK1, p38, and ERK1/2 are activated by MKKs, causing nuclear translocation of AP-1. 4. As a result of TLR4 activation, there is increased release of proinflammatory cytokines which leads to inflammation, cardiac dysfunction, and eventually death.

1.4 Mitogen-activated protein kinases in sepsis

Mitogen-activated protein kinases (MAPKs) are a group of serine/threonine protein kinases with three well-delineated subfamilies, including extracellular-signal-regulated kinase (ERK) 1/2, the c-Jun NH2-terminal kinases (JNK) and p38 kinases. MAPK pathway signaling is induced by upstream receptor activation, including GPCR and TLR4. MAPKs' activities are regulated by their phosphorylation levels. Each MAPK can be phosphorylated by upstream kinases including mitogen-activated protein kinase kinase (MKKs), as well as PKA and PKC.⁵⁸ Upstream activity of MAP kinase kinase kinase (MAP3K) activates MKK in a sequential phosphorylation cascade to trigger MAPK signaling.⁵⁹ Regulation of substrates downstream of MAPK activity modulates cellular pathways in proliferation, differentiation, inflammation, and apoptosis.⁵⁵ Inactivation of MAPK signaling is mediated by MAPK phosphatases (MKPs), which dephosphorylate both the threonine and tyrosine residues.⁶⁰

MAPKs are mediators in LPS-induced TNF- α production (Figure 1.1).^{26,61,62} Activation of MAPKs and Akt in the heart during sepsis causes cardiac dysfunction in mice.⁶³ In the latter study, left ventricular cardiomyocytes and macrophages showed activation of MAPKs under septic conditions. Our lab previously elucidated specific roles for MAPKs in the regulation of myocardial TNF- α expression during sepsis, showing that gp91phox-containing nicotinamide adenine dinucleotide phosphate (NADPH) oxidase signaling contributes to LPS-stimulated TNF- α expression in cardiomyocytes.^{64,65} This effect was facilitated through p38 and ERK1/2 MAPK signaling pathways.⁶⁵ ERK has two ubiquitously expressed isoforms, ERK1/2, and is involved in regulation of inflammatory cytokine synthesis.⁶⁶ The p38 MAPK α isoform is targeted by endotoxins in mammalian cells.⁶⁷ It has a regulatory role in inflammatory cytokine release via both transcriptional and post-transcriptional mechanisms.⁶⁸ p38 MAPK activity is also regulated by Gas-induced cAMP signaling pathways and Gq-PLC β pathways.^{69,70}

LPS can also induce myocardial MKP1 expression via JNK1. MKP1 attenuates ERK1/2 and p38 activation, which inhibits myocardial TNF- α expression during endotoxemia.⁷¹ ERK1/2 and JNK are important in many cellular pathways; ERK1/2 activity can be modulated by upstream G protein signaling, and JNK activation can be activated by Gi-

and Gq-stimulated pathways and suppressed by cAMP signaling.^{70,72} As c-Jun is a part of the activator protein-1 transcription factor (AP-1), which regulates the expression of proinflammatory cytokines, JNK is involved in inflammatory response pathways.⁷³ Increased expression of JNK/c-fos resulted in lower phosphorylation of ERK1/2 and p38, which leads to lower TNF- α expression in LPS-stimulated cardiomyocytes.⁶¹

1.5 NF- κ B in inflammatory signaling

The nuclear factor of kappa light polypeptide gene enhancer in B-cells (NF- κ B) is an inducible transcription factor that plays a central role in physiological and pathological conditions.⁷⁴ While it exhibits a constitutive background activity, the pathway is inducible by factors including cytokines, toll-like receptor ligands, and bacteria. The NF- κ B family consists of members that form dimeric transcription factors, and these bind to specific DNA targets known as κ B binding sites. κ B binding sites are present in promoter and enhancer regions of a multitude of genes.⁷⁵ When inactive, NF- κ B is found in the cytoplasm bound and inhibited by nuclear factor of kappa light polypeptide gene enhancer in B-cells inhibitor (I κ B) proteins, which masks the nuclear translocation sequence. When induced, the canonical activation of NF- κ B involves the phosphorylation of I κ B α by I κ B kinases (IKK), leading to its degradation.^{76,77} IKK activity can be triggered by cytokines, mitogens, stress factors, and microbial components.⁷⁸ Following I κ B α degradation, NF- κ B members, mainly p50/p65 dimers, translocate to the nucleus.⁷⁶ Activation of NF- κ B increases the presence of nuclear DNA-binding subunits, which bind to specific κ B binding sites to regulate the expression of target genes.

This canonical pathway of NF- κ B activation is responsible for TLR-mediated expression of inflammatory cytokines such as TNF- α and IL-6.⁷⁵ TLR4 activation can induce NF- κ B activity through two signaling pathways (Figure 1.1). Briefly, through activation of interleukin-1 receptor associated kinases (IRAKs) and recruitment of transforming growth factor- β -activated kinase-1 (TAK1), MyD88 can mediate the activation of the IKK complex as well as MAPKs. In MyD88 deficient mice and cells, TLR activation is able to induce neither NF- κ B activity nor inflammatory cytokine expression in response to LPS.⁷⁹ In addition, TLR4 induces NF- κ B activity through a TRIF-dependent pathway, resulting

in a corresponding expression of inflammatory cytokines. This pathway converges with the MyD88-dependent path through a similar activation of TAK1.⁷⁵ TAK1 deficient cells have lower levels of NF- κ B and MAPK activity, resulting in impaired inflammatory response.⁸⁰ Similarly, in TRIF-deficient cells, early LPS activation of NF- κ B is still present.⁸¹ In contrast, when both MyD88 and TRIF are knocked out, there is a complete absence of NF- κ B activity when stimulated by LPS.⁸¹ Thus, TLR4 mediated inflammatory response through the activation of NF- κ B is reliant on both the MyD88 and TRIF pathways.

NF- κ B is a central mediator of proinflammatory cytokine expression and can prolong inflammatory conditions through a feed-forward loop via IKK activity.^{77,82} IKK phosphorylates I κ B proteins to activate the NF- κ B transcription factors. A substrate of IKK is the E3 ubiquitin ligase Itchy homolog, ITCH, which is involved in the suppression of TNF-mediated NF- κ B activation. ITCH activity is impaired when it is phosphorylated by IKK, which prolongs NF- κ B signaling and proinflammatory cytokine release, such as TNF- α .⁸²

1.6 G protein-coupled receptors

G protein-coupled receptors (GPCRs), which have seven transmembrane domains, are the largest membrane receptor family. They are involved in diverse physiological and disease processes. GPCRs transduce signals from a multitude of molecules including hormones, neurotransmitters, chemokines, and autocrine and paracrine factors.⁸³

Signal transduction in mammalian cells is regulated by mechanisms that amplify or attenuate agonist-initiated biochemical cascades.⁸⁴ As shown in Figure 1.2, the G α -subunit in the inactivated state typically is found bound to guanosine diphosphate (GDP). When a GPCR is activated by a ligand, GDP is exchanged for guanosine triphosphate (GTP) on the receptor-associated G α -subunit. This results in a conformational rearrangement and likely the dissociation of G $\beta\gamma$ -subunit from the G α -subunit. Both subunits can activate downstream messenger cascades. Eventually, the intrinsic GTPase activity of the G α -subunit catalyzes the hydrolysis of GTP to GDP. The inactive heterotrimeric G protein complex then re-forms, and G protein signaling is abrogated.⁸⁵

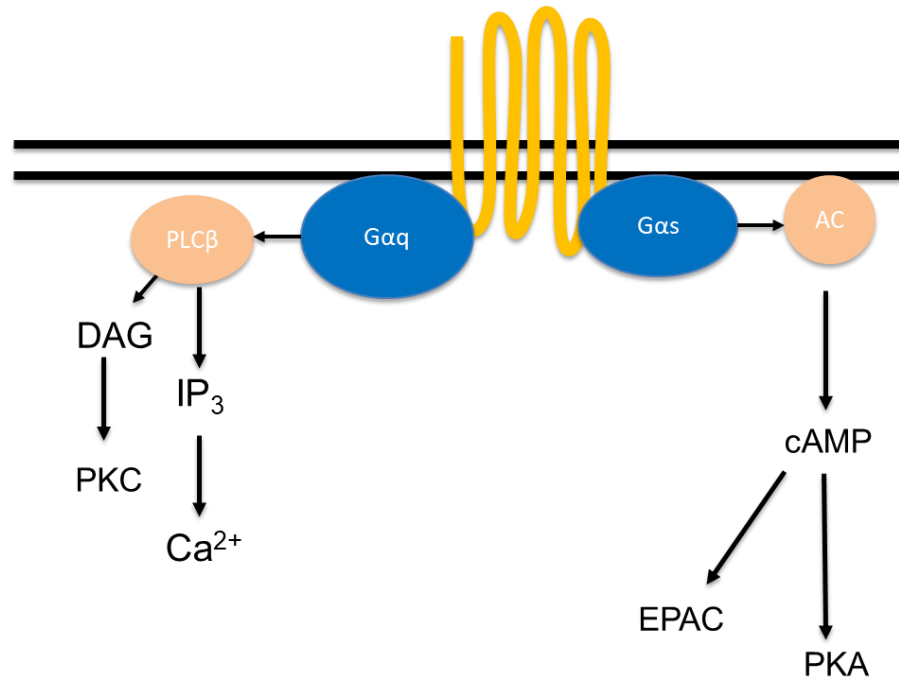


Figure 1.2. Conventional signaling pathways of *Gαs* and *Gαq* activity. Upon activation, *Gαq* stimulates phospholipase Cβ (*PLCβ*) to cleave *PIP*₂ to the second messengers inositol trisphosphate (*IP*₃) and diacylglycerol (*DAG*). *IP*₃ increases intracellular *Ca*²⁺ concentration by inducing *Ca*²⁺ release from the endoplasmic reticulum. *DAG* activates protein kinase C (*PKC*). *Gαs* stimulates adenylyl cyclase (*AC*) to produce the second messenger *cAMP*, which activates protein kinase A (*PKA*). This results in the phosphorylation of many intracellular proteins and affects many intracellular pathways.

G proteins can be sorted into four classes depending on their G α -subunits: G α stimulatory (G α s), G α inhibitory (G α i), G α q and G α 12/13.⁸⁶ The different classes and subunits, when activated, trigger a variety of distinct pathways. As shown in Figure 1.2, activated G α s stimulates adenylyl cyclase to produce the second messenger cyclic adenosine monophosphate (cAMP), which in turn activates protein kinase A (PKA) as well as exchange protein directly activated by cAMP (EPAC) and cyclic nucleotide-gated ion channels such as hyperpolarization-activated cyclic nucleotide-gated (HCN) channels in cardiac pacemaker cells.⁸⁷ When activated, PKA is able to phosphorylate other intracellular proteins and affect many intracellular pathways. Opposing the actions of G α s, G α i inhibits adenylyl cyclase activity to limit the production of cAMP.⁸⁸ G α q stimulates phospholipase C β (PLC β) as well as the small G protein nucleotide exchange factor p63RhoGEF.⁸⁹ Activated PLC cleaves phosphatidylinositol 4,5 - bisphosphate (PIP₂) to yield the second messengers inositol 1,4,5 - triphosphate (IP₃) and diacylglycerol (DAG). IP₃ increases Ca²⁺ release from the endoplasmic reticulum, and thus enhances Ca²⁺ concentration. DAG and IP₃ can activate protein kinase C (PKC), either directly or indirectly via the release of Ca²⁺, respectively.^{70,83} This results in downstream phosphorylation of proteins to modulate intracellular pathways.⁸⁸

1.6.1 G-protein signaling regulates MAPK activity

When activated, G proteins regulate signal transduction via mechanisms that intensify or mitigate cellular pathways, including the activation of MAPKs via activation of small, Ras-like G proteins, modulation of the MAPK phosphorylation cascade or transactivation of receptor tyrosine kinases.^{70,84} G α s stimulates ERK1/2 and p38 signaling via its activation of cAMP production. Specifically, cAMP activation of EPAC stimulates Rap-1 signaling, which is capable of inducing b-Raf, a MAP3K, upstream of ERK1/2.^{90,91} However, the EPAC-dependent activation of ERK1/2 via Rap-1 is cell specific.⁹² cAMP-mediated PKA activity is also involved as an upstream regulator of ERK1/2 via Rap-1. PKA-mediated upstream regulation of ERK1/2 is cell type dependent and can amplify and/or attenuate the MAPK activity. For example, PKA is involved in agonist-stimulated ERK1/2 activation via Ras in human embryonic kidney cells, while in arterial smooth muscle cells, PKA inhibited the upstream signaling of MKK.^{93,94} In cardiomyocytes, PKA can also target

Ca²⁺-handling proteins.⁹⁵ Similar to the G_{αs} induced ERK1/2 MAPK, β₂-AR activation mediated the G_{αs}-cAMP–PKA stimulation of p38 signaling in cardiomyocytes.⁹⁶ Gi mediates MAPK activity through its α-subunit as well as βγ-subunit.⁷⁰ In fibroblast cells, G_{αi} can activate ERK1/2 signaling through direct or indirect stimulation of Ras.⁹⁷ G_{αi} is known to inhibit AC activity, reducing cAMP levels. This decrease alleviates the inhibitory effect of PKA on upstream c-Raf, which enhances ERK1/2 signaling.⁷⁰ G_{αi} also activates ERK1/2 and JNK directly through βγ-subunit dependent mechanism and indirectly via PI3K activity.⁹⁸

Finally, G_{αq} mediates MAPK signaling via activation of PLCβ.⁷⁰ The effector PLCβ can be activated by the G_{αq}-subunit, and the βγ-subunit can enhance the effect of the G_{αq}-subunit.⁹⁹ Upon activation, PLCβ activates PKC and increases intracellular Ca²⁺ levels, both which induces ERK1/2, JNK, and p38 MAPK signaling.⁷⁰ G_{αq} stimulated PKC can phosphorylate c-Raf, upstream of ERK1/2. Additionally, G_{αq} can induce ERK1/2 via a Ca²⁺-calmodulin mediated pathway, while both DAG and Ca²⁺ can activate Rap-1 to enhance ERK1/2 activity.¹⁰⁰ Lastly, G_{αq} mediates p38 activity through PKC signaling or βγ-subunit activated Rap-1 pathways.¹⁰¹ Thus, GPCR activity may be involved in the inflammatory response in sepsis via the MAPK pathways.

1.6.2 G protein signaling in sepsis

Cardiovascular function including cardiac contractility, heart rate and vascular tone, etc. is regulated by GPCR signaling. The receptor family can be found in different cells involved in the cardiovascular system, including cardiomyocytes, fibroblasts, and endothelial cells. As such, GPCRs are widely used therapeutic targets for pharmacological treatment including angiotensin converting enzyme (ACE) inhibitors, and β-AR ligands.¹⁰² For example, dobutamine is a selective adrenergic receptor agonist and an inotropic agent for the treatment of cardiogenic shock.¹⁰³

The initial phase of sepsis is identified by increased catecholamine levels as a part of the compensatory adrenergic response to alleviate myocardial depression.¹⁰⁴ In the long term however, this excessive stimulation of cardiac β-AR and intracellular Ca²⁺ levels may be detrimental for the heart, resulting in myocardial damage, cardiac dysfunction, tachycardia,

and apoptosis.¹⁰⁵ β_2 -AR can also stimulate Ca^{2+} release from intracellular stores via PLC and opening of IP_3 receptors, which does not involve the canonical β_2 -AR-GPCR signaling pathways.¹⁰⁶ Additionally, desensitization and downregulation of β -AR is associated with sepsis progression, which may be caused by prolonged cytokine expression.¹⁰⁷ Chronic elevations of catecholamines also activate α_1 -AR in the heart, which contributes to contractility via $\text{G}\alpha_q$ signaling.¹⁰⁸ In contrast to the downregulation of β -AR, α_1 -AR activity is maintained during heart failure.^{109,110}

Adenylyl cyclase (AC) activity is reduced in the late hypodynamic stage of sepsis, though this may be isoform dependent as AC4 expression was enhanced in the heart.^{111,112} Enhanced phosphodiesterase (PDE) activity during sepsis may also contribute to the desensitization of β -AR stimulation. Dobutamine's inotropic effect was impaired in sepsis.¹¹³ While surface expression levels of β_1 -adrenoceptors and α -subunits of three main G protein families in the myocardium were not different from control, plasma cAMP levels were lower as a result of upregulated PDE4D expression.¹¹³ Endotoxemia can also induce a systemic downregulation of α_1 -AR expression, which may contribute to circulatory failure in sepsis.¹¹⁴ Similarly, $\text{G}\alpha_s$ induced production of mitochondrial cAMP was impaired in the myocardium in sepsis.¹¹⁵

$\text{G}\alpha_i$ signaling may also contribute to negative inotropic effect of LPS in cardiomyocytes.¹¹⁶ As well, adrenergic receptors modulate inflammation and the immune response. Stimulation of α_2 -adrenoceptor *in vivo* resulted in higher proinflammatory cytokines release, including $\text{TNF-}\alpha$.^{117,118} In contrast, treatment of dexmedetomidine, an α_2 -adrenoceptor agonist, alleviated septic renal dysfunction and lowered the expression of proinflammatory cytokines (*e.g.* $\text{TNF-}\alpha$).¹¹⁹ However, this effect may be due to the renal specific and initial effects of the drug, which reduces the sympathetic response and catecholamine release, alleviating inflammation.^{119,120} Currently, norepinephrine, which targets adrenergic receptors, is the first-line recommendation for treatment of septic shock.¹² Thus, G protein signaling is involved in septic conditions.

1.7 Regulators of G protein signaling

Regulator of G protein signaling (RGS) are expressed in many tissues and are involved in diverse physiological and disease processes. They function as GTPase-activating proteins (GAPs) for G protein α -subunit through a conserved ~120 amino acid RGS domain.^{121,122} As GAPs, RGS proteins increase the rate of hydrolysis of the $G\alpha$ -subunit-bound GTP, inhibiting downstream signaling pathways. As well, at least some RGS proteins can act through GAP-independent mechanisms to limit GPCR signaling. For example, RGS2 not only promotes $G_{\alpha s}$ GTPase activity but also acts as an “effector antagonist” by binding to $G_{\alpha s}$ and/or AC to limit GPCR-stimulated cAMP production, as well as $G_{\alpha q}$ -mediated PLC β activation (Figure 1.3).^{123–126} Thus, RGS limits GPCR signaling through both GAP-dependent and -independent mechanisms.

In mammals, there are currently twenty identified RGS genes and some of these encode multiple splice variants. These proteins and their splice variants can be further categorized into four subfamilies: R4/B, RZ/A, R7/C, and R12/D.¹²⁴ The predominant RGS proteins expressed in the cardiovascular system are the small RGS R4/B subfamily members, RGS2-5.¹²⁷ Additionally, R7/C subfamily member RGS6 is also found in the ventricles and is considered to be cardioprotective.¹²⁸ These RGS proteins are prevalent in mammalian hearts and expressed in cardiomyocytes and fibroblasts.^{129–131} RGS2-4 have altered expression profiles in human heart failure.^{130,132} In the heart, RGS4 and RGS5 are predominantly expressed in the atria, while RGS2 is highly expressed in the ventricles.^{127,129} Thus, targeting RGS2 therapeutically has the potential to be clinically beneficial.^{133,134}

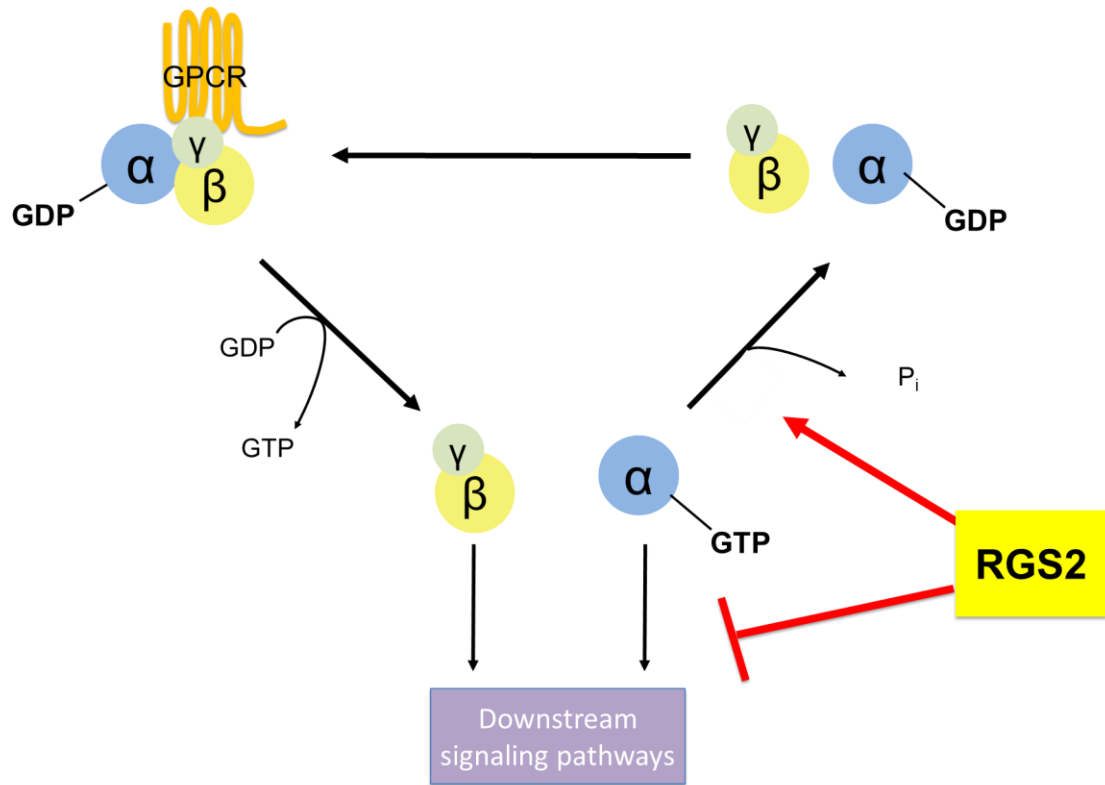


Figure 1.3. RGS2 regulation of G protein signaling . Under basal conditions, $G\alpha$ has a GDP bound to it. Upon activation of the GPCR, GDP-GTP exchange on $G\alpha$ is thought to cause the separation of $G\alpha$ from $G\beta\gamma$, allowing receptor-mediated activity and initiating downstream signaling cascades. RGS2 increases the intrinsic GTP hydrolytic activity of $G\alpha$. This GAP effect attenuates $G\alpha$ activity and results in a return to the ground state of the heterotrimeric G protein subunits. This also stops $G\beta\gamma$ signaling activity. As well, RGS2 can act through GAP-independent activity as an effector antagonist binding adenylyl cyclase (AC) and $G\alpha_s$ -mediated cAMP production, as well as $G\alpha_q$ -mediated phospholipase $C\beta$ signaling.

1.7.1 Regulator of G protein signaling 2

In addition to being expressed in the heart, RGS2 is detected throughout the body, including the brain, vasculature, and kidneys. As part of the R4/B subfamily, it has a relatively small and simple structure. It preferentially targets Gαq- and Gαs-mediated pathways which are implicated in blood pressure regulation and cardiac hypertrophy.^{135,136} RGS2 is unique in its relatively low affinity for Gαi/o proteins, due to its conformation and/or sequence in its binding pocket.¹³⁷ GPCRs can also recruit RGS2 to the plasma membrane without the requirement of receptor activation.¹³⁸ The region between the RGS domain and the N-terminus has been shown to selectively target the M1 muscarinic acetylcholine receptor, α_{1A} and β₂-adrenergic receptors.^{123,139,140} Previous studies also identified a 37 amino acid binding domain (RGS2^{eb}) within the RGS2 domain that binds eIF2Bε, which inhibits global protein synthesis.^{141,142} Additionally, a point mutation in RGS2 inhibited its GAP activity but did not affect RGS2 translational control. This shows that the mechanism by which RGS2 is able to reduce protein synthesis is also independent of its modulation of GPCR activity.¹⁴²

RGS2 activity can be modulated by phosphorylation, which is facilitated by PKC and type I α cGMP-dependent protein kinase (cGKIα), to increase RGS2's GAP-dependent activity.^{143,144} As well, proteolytic degradation of RGS2 affects its downstream inhibition of GPCR signaling.¹⁴⁵ Inhibition of cGK activity limits RGS2 degradation.¹⁴⁴ RGS2 also attenuates Gαq-coupled vasoconstriction in vascular smooth muscle.¹⁴⁶ Gαq has been shown to be involved in myocardial hypertrophy – Gαq-coupled receptors exert diverse effects on myocyte growth, contractility, and heart rate.¹⁴⁷ In addition, Gαq contributes significantly to the maladaptive remodeling that results from pressure overload.¹⁴⁸

Finally, RGS2 deficient mice exhibit a strong hypertensive phenotype, renovascular abnormalities, and prolonged response to vasoconstrictors *in vivo*.¹⁴⁹ These mice are more likely to have atrial fibrillation caused by increased M3 muscarinic receptor activity, which is associated with increases in higher vagal tone and is predominantly coupled to Gαq class of G proteins.^{150,151} Additionally, RGS2 deficiency resulted in a hypertensive mice, and pressure overload leads to hypertrophy, heart failure, and death.^{136,149,152} Clinical cases of hypertensive patients have decreased RGS2 mRNA and protein levels.^{132,153} In contrast,

hypotension is a symptom of Bartter's/Gitelman's syndrome, in which patients have increased RGS2 expression.¹⁵⁴

RGS2 expression is also altered in cardiovascular disease models. For example, RGS2 is downregulated in cardiac hypertrophy and heart failure models. As well, there is an acute enhancement of its expression in response to GPCR agonists that promote hypertrophy in cardiomyocytes.^{135,155,156} Correspondingly, sustaining RGS2 expression improves cardiac hypertrophy *in vitro* and *in vivo*.^{134,157} By upregulating RGS2 protein levels, digoxin was cardioprotective against cardiac hypertrophy and injury *in vivo*; this effect was absent in RGS2 deficient mice.¹⁵⁷ Similarly, lower levels of RGS2 and higher angiotensin II mediated MAPK activity was detected in hypertensive patient samples of human skin fibroblasts and peripheral blood mononuclear cells.¹⁵⁸ Thus, RGS2 has a regulatory role in the heart and is a pharmacological target in the treatment of cardiovascular diseases.¹⁵⁷ Currently, its role in sepsis is unclear.

1.8 Summary and rationale

While both the LPS-stimulated TLR4 and the RGS2-regulated GPCR pathways are well established, no studies to date have investigated how these two interact in the heart. RGS2 has been suggested to inhibit MAPKs, including p38, ERK1/2, and JNK (Figure 1.4).⁶² Notably, these mediators have been implicated in proinflammatory cytokine release in endotoxemia. Crosstalk among JNK, p38 and ERK is another important feature in MAPK signaling. JNK1 suppresses TNF- α expression in LPS-stimulated cardiomyocytes.⁶¹ Inhibition of TNF- α expression by JNK1 signaling is mediated by c-fos induction and down-regulation of ERK and p38 phosphorylation. This negative crosstalk between JNK1 and ERK/p38 signaling may limit TNF- α expression in sepsis. Furthermore, it has been demonstrated that inhibition of p38 activation decreases TNF- α expression in the heart and improves cardiac function and survival during endotoxemia.³³ This also suggests an important role for p38 in the development of cardiac dysfunction in sepsis. Thus, RGS2 may be able to regulate the release of proinflammatory cytokines through modulating MAPK phosphorylation.

Induced activation of NF- κ B may be downstream of MAPK signaling. Additionally, NF- κ B was shown to be involved in a feedforward loop that exacerbates inflammatory conditions (Figure 1.4).⁸² TLR4 activation induces further downstream IKK complex activity.⁴² RGS2 may further modulate kinase activity by limiting the downstream activity of PKC.¹⁵⁹

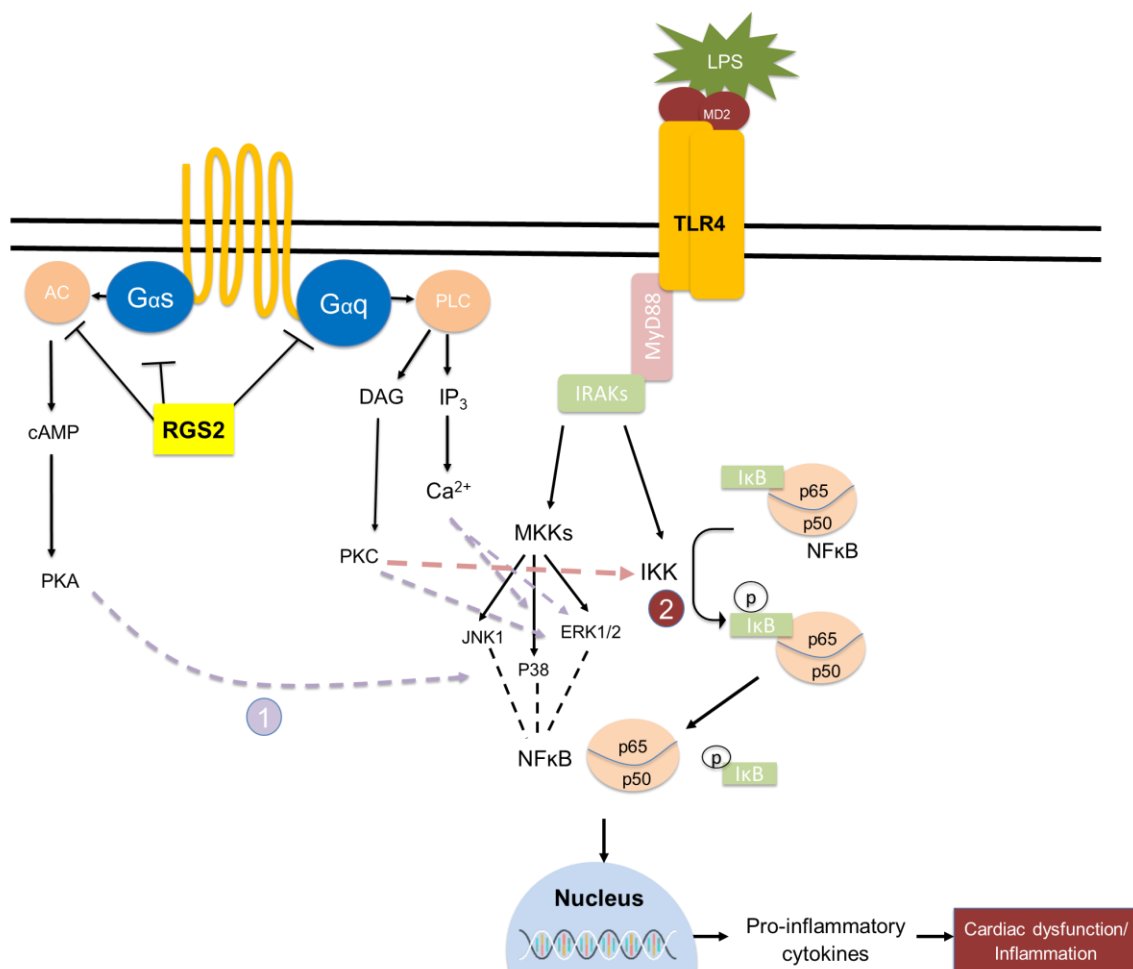


Figure 1.4. Possible crosstalk mechanisms involving the role of RGS2 in limiting G protein signaling activity. 1. RGS2 may inhibit LPS-induced expression through downregulation of mitogen-activated protein kinases (MAPKs) p38, ERK1/2, and JNK, which are implicated in proinflammatory cytokine release in endotoxemia. 2. TLR4 regulates downstream IKK complex activity. RGS2 may further modulate kinase activity by downstream regulation by protein kinase C. All signaling pathways result in the production of proinflammatory cytokines, leading to inflammation and cardiac dysfunction.

1.9 Hypothesis and aims

This study investigated how global RGS2 deficiency affects inflammatory cytokine release within the heart and elucidated its mechanism of action during endotoxemia.

We hypothesized that RGS2 deficiency would enhance the proinflammatory response in endotoxemia.

The specific objectives of the study were:

- 1) To determine the role of RGS2 in LPS-induced inflammatory cytokine (*e.g.* TNF- α) release in the heart.

Adult male wild-type (WT) and *RGS2*^{-/-} C57BL/6 mice were used as our control and RGS2 deficient models, respectively, which have been used in previously in our lab.^{151,160,161} These mice were treated with LPS (4 mg/kg) by intraperitoneal (IP) injection; previous studies showed that the dosage is sufficient to induce endotoxemia to model septic conditions.⁶¹

While the *in vivo* model allowed us to understand the physiological relevance of RGS2, studying molecular and cellular mechanisms required isolated cells, which avoided the complexity of whole animal studies. Thus, we complemented our *in vivo* model with an *in vitro* primary neonatal mouse cardiomyocyte model. This isolated model allowed studying the specific role of RGS2 in cardiomyocytes in septic conditions.

To determine the physiological role of RGS2 in inflammatory cytokine release under endotoxemic conditions, inflammatory cytokine levels, including TNF- α , IL-6, and IL-1 β were assessed. As well, we detected altered cardiac function using echocardiography.

- 2) To identify specific pathways regulated by RGS2.

To determine specific mechanism through which RGS2 affects during endotoxemia, we detected the phosphorylation of pathway mediators by immunoblotting. These included

ERK1/2 and p38 MAPKs. Relative NF- κ B activity was detected via ELISA. Finally, the signaling mediator PKA was inhibited using a selective inhibitor H89 and changes in LPS-induced inflammatory response were assessed.

Chapter 2

2 Materials and Methods

2.1 *In vivo* C57BL/6 mouse model

This study utilized mice in accordance with the Guidelines for the Care and Use of Animals by the Canadian Council of Animal Care. The study protocol was approved by the Animal Care Committee at Western University, Canada (AUP #2016-099, Appendix A). Wild-type (WT) C57BL/6 mice were purchased from Jackson Laboratory (Bar Harbor, Maine). Generation of *RGS2*^{-/-} mice have been previously described.^{162,163} Mice were given water and chow *ad libitum* and held on a 12h-12h light-dark cycle. All mice used were 3-5 months old males. Female mice were not used in the present experiment to avoid sex-dependent differences in the inflammatory response during endotoxemia, which may be affected by the estrous cycle.^{164,165}

2.1.1 LPS-induced endotoxemia mouse model

WT and *RGS2*^{-/-} mice were treated with saline as control or 4 mg/kg LPS by intraperitoneal (IP) injection to induce endotoxemia. Plasma and left ventricular tissues were collected 0.5, 2, 4, or 24 hours after injection. LPS treatment periods were previously established in our lab.^{61,71} Blood was collected by cardiac puncture in heparinized needles and tubes. Plasma was isolated from blood by centrifugation at 5,000 x g for 5 minutes at 4 °C, and the top layer of plasma was transferred to a new tube. The left ventricle (LV) of the heart was isolated and collected. All samples were stored at -80 °C until analysed.

2.2 Primary neonatal cardiomyocyte cell culture

2.2.1 Isolation of neonatal cardiomyocytes

Primary cultures of neonatal mouse cardiomyocytes were used according to methods previously described, with minor adjustments.^{160,166,167} Male and female WT and *RGS2*^{-/-} neonates (P0) were sacrificed and sterilized rapidly in clinicide (Vetoquinol, Lavaltrie, Québec). Using sterilized tools, neonatal ventricles were collected and washed in D-Hanks solution (H2389, Sigma, St. Louis, Missouri). Ventricles were cut into 4-6 pieces/heart and

incubated in neonatal heart digestion buffer (Liberase TH, Roche; 22.5 µg/mL in D-Hanks solution) at 37 °C for 15 minutes. Digestion buffer for the first digestion incubation was removed, and fresh digestion buffer was added. Ventricles were incubated for 15 minutes with occasional gentle shaking. Digested ventricles were then broken down mechanically by thorough triturating of the tissue to release cells. The supernatant, which contained cells, was transferred to a new tube and centrifuged at 180 x g for 4 minutes at room temperature. Cells were re-suspended in neonatal cardiomyocyte culture media (M199 media, 10% fetal bovine serum FBS, 1% penicillin/streptomycin, 1% L-glutamine) and pre-plated on a sterilized cell culture dish. Fresh digestion buffer was added to the ventricles and digestion was repeated two more times, for a total of four digestion incubations (1 hour total). After the final digestion, pre-plated cells were incubated for 45 minutes to allow fibroblasts to strongly adhere to the bottom of the plate.

Weakly adhered cardiomyocytes were then gently washed off the dish and isolated from the adhered fibroblasts, filtered via gravity to remove any large tissue debris, and re-suspended in neonatal cardiomyocyte culture media. Neonatal cardiomyocytes were seeded on 1% gelatin coated plates. Neonatal cardiomyocytes were incubated at 37 °C with 5% CO₂ for 48 hours prior to treatment. Overall health of neonatal cardiomyocytes was confirmed via microscopy to detect overall abundance of cells and cardiomyocyte contraction. Quality of cultured cardiomyocytes was confirmed by immunohistochemistry.

2.2.2 LPS-induced inflammatory cytokine release in cardiomyocytes

Neonatal cardiomyocyte cultures were washed briefly with sterile phosphate buffered saline (PBS), and fresh cardiomyocyte culture medium was added. Cells were treated with medium as control, and LPS (5 µg/mL) for 0.5, 2, and 4 hours at 37 °C with 5 % CO₂. LPS treatment periods were previously established.^{61,71} At the end of the treatment period, media and cardiomyocyte cells were collected and stored at -80 °C.

2.2.3 PKA inhibition in LPS-induced inflammatory cytokine release

PKA inhibitor H89 was used to pre-treat cardiomyocyte cultures prior to LPS treatment. After the 48 hours incubation period, cardiomyocyte cultures were washed with PBS. H89 was added to achieve 20 µM in cardiomyocyte culture medium for 30 minutes of pre-

treatment. DMSO was used as control. After pre-treatment, LPS (5 $\mu\text{g}/\text{mL}$) was added directly to the cardiomyocyte culture media for 2 and 4 hours at 37 °C with 5% CO_2 . Media and cardiomyocyte cells were collected and stored at -80 °C.

2.2.4 Immunohistochemistry of cardiomyocytes

Cultured neonatal cardiomyocyte cells were seeded on 1% laminin-coated glass slide after the pre-plating period. Cells were incubated at 37 °C with 5% CO_2 for 48 hours. Prior to fixation, cells were washed with PBS. Cardiomyocytes were fixed with cold 100% methanol for 15 minutes at 4 °C, then briefly washed with PBS.

Purity of the cardiomyocyte culture was confirmed by α -actinin staining to identify cells that were cardiomyocytes. Fixed cells were blocked for 1 hour at room temperature in goat serum, then incubated in primary α -actinin antibody (1:1,000; #A7811, Sigma, St. Louis, MO) overnight at room temperature in a humidity chamber. Cells were washed with PBS, then incubated in secondary antibody (1:1,000 Cy3-conjugated goat anti-mouse IgG; Jackson ImmunoResearch, PA) for 1 hr. Cells were briefly washed with PBS, then nuclei were stained using Hoechst 33342 stain (1:1,000 Invitrogen, Carlsbad, CA) for 10 minutes. A glass coverslip was mounted on the slide, and the cells were imaged using fluorescence microscopy (Figure 2.1).

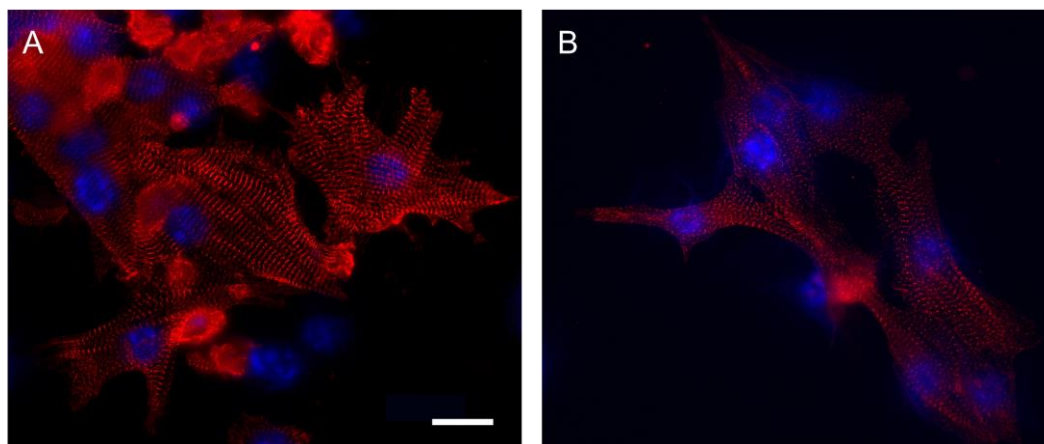


Figure 2.1: Efficacy of the isolation of neonatal cardiomyocytes. Representative fluorescent image of fixed WT (A) and *RGS2*^{-/-} (B) mouse primary neonatal cardiomyocytes stained for α -actinin (red) and Hoechst stain (blue) for detection of the nucleus. Scale bar (white) = 20 μ m. More than 90% of stained cells were identified as cardiomyocytes.

2.3 Quantitative polymerase chain reaction

2.3.1 RNA isolation from LV tissues

RNA was collected from tissue samples using TRIzol reagent (Invitrogen). Briefly, left ventricle samples collected from WT and *RGS2*^{-/-} mice treated with LPS (4 mg/kg) or saline for 2 hours treated were washed in ice cold PBS, then mechanically homogenized using a Model PRO 200 (PRO Scientific Inc., Monroe, CT USA) in 500 μ L/sample TRIzol. Chloroform was added (1/5 of TRIzol volume; 100 μ L/sample) and samples were vortexed vigorously. After 10 minutes at room temperature, the samples were centrifuged at 12,000 x g at 4 °C for 15 minutes. The aqueous top layer containing the RNA was transferred to a new tube, and isopropanol was added (1/2 of TRIzol volume; 250 μ L/sample). Samples were briefly vortexed, then incubated at room temperature for 10 minutes. The sample was centrifuged at 12,000 x g at 4 °C for 10 minutes to pellet the precipitated RNA. The supernatant was removed, and the RNA pellet was washed superficially using 75% ethanol in 0.1% DEPC water (same as TRIzol volume; 500 μ L/sample). The sample was again centrifuged at 12,000 x g at 4 °C for 10 minutes. Ethanol wash was removed, and RNA pellet was air dried until no liquid remained (about 30 minutes). The RNA pellet was

resuspended in 0.1% DEPC water, then heated to 65 °C for 10 minutes. RNA quality and quantity were assessed using the NanodropLite spectrophotometer (Thermo Fisher Scientific, Waltham, Massachusetts).

2.3.2 RNA isolation from cardiomyocytes

Cardiomyocyte cells treated with LPS for 2 hours were washed with ice cold PBS, and then lysed using TRIzol reagent (500 µL/sample) on ice. RNA was isolated using the TRIzol reagent method, as described above.

2.3.3 Reverse transcription

After RNA isolation, reverse transcription was performed using the quantified RNA samples. RNA was diluted in 0.1% DEPC water for a total of 0.5 µg of RNA in 11.5 µL. Random primers (20 µM) were added in the mixture (1 µL) and heated to 65 °C for 5 minutes, followed by cooling on ice for 3 minutes. Reverse transcription master mix (4 µL of 5x FirstStrand buffer, 2 µL of 0.1 M DTT, 1 µL of 10 mM dNTP, and 0.5 µL of 200 U/µL M-MLV reverse transcriptase) was then added to each sample. Samples were incubated at 37 °C for 4 hours. M-MLV reverse transcriptase was inactivated by incubating the cDNA mixture at 95 °C for 5 minutes, and cDNA was stored at -20 °C for subsequent qPCR.

2.3.4 Quantitative real-time PCR

Following reverse transcription, the resulting cDNA was diluted with water, and then incubated at 65 °C for 5 minutes. Real-time quantitative PCR amplification was performed for each cDNA sample using: 2.5 µL ddH₂O, 5 µL 2x EvaGreen qPCR MasterMix, 0.5 µL of primer for gene of interest (Forward + Reverse; 20 µM), and 2 µL of cDNA. The internal control gene was 28S ribosomal RNA. For 28S rRNA detection, the cDNA was diluted 500 times. Primers were designed to amplify the target genes, as shown in Table 2.1. Eppendorf MasterCycler Realplex² (Eppendorf, Hamburg, Germany) was used to amplify qPCR mixtures for 35 cycles. The standard curve method was used to derive the gene of interest mRNA content. The relative mRNA quantity of target genes to the internal control were derived using a comparative C_T method.

Table 2.1. Forward and reverse primer sequences and specific annealing temperature for genes of interest.

Gene of interest (Accession #)	Annealing Temperature	Primer sequence
<i>TNF-α</i> (NM_013693.3)	61 °C	Forward 5'-CGGCATGGATCTCAAAGACA-3' Reverse 5'-CTTGACGGCAGAGAGGAGGT-3'
<i>28S</i> (NR_003279.1)	61 °C	Forward 5'-GCCTCACGATCCTTCTGACC-3' Reverse 5'-AACCCAGCTCACGTTCCCTA-3'
<i>IL-6</i> (NM_031168.2)	61 °C	Forward 5'-CAAAGCCAGAGTCCTTCAGAG-3' Reverse 5'-ATGGTCTTGGTCCTTAGCCAC-3'
<i>IL-1β</i> (NM_008361.4)	63 °C	Forward 5'-ACAAGGAGAACCAAGCAACGA-3' Reverse 5'-GCTGATGTACCAGTTGGGGAAC-3'
<i>RGS2</i> (NM_009061.4)	60 °C	Forward 5'-CATTTGATGAACTGCTGGCCA-3' Reverse 5'-GCAGCCACTTGTAGCCTCTT-3'

2.4 TNF- α ELISA

Inflammatory cytokine TNF- α levels in plasma and cell media treated with vehicle or LPS for 4 hours were detected using Mouse TNF α ELISA Ready-SET-Go kit (eBioscience, San Diego, California), following the manufacturer's protocol.

Total protein levels in cardiomyocyte cultures were determined by Lowry protein assay. The protein standard curve was extrapolated from bovine serum albumin (BSA) standards. Samples were read using a SpectraMax M5 (Molecular Devices, San Jose) and SoftMax Pro software. TNF- α levels in the cardiomyocyte culture media were normalized to total protein levels.

2.5 NF- κ B activity

2.5.1 Nuclear protein extraction

WT and *RGS2*^{-/-} mice were treated with LPS or saline (4 mg/kg, IP) for 0.5 hour. Left ventricles were collected and used in the extraction of nuclear protein. To each tissue sample, 800 μ L of Buffer A (10 mM HEPES pH7.9, 1.5 mM KCl, 10 mM MgCl₂, 0.5 mM DTT, 0.1% NP40, 1 mM PMSF) was added. Tissues were homogenized using a mechanical homogenizer, and samples were incubated on ice for 30 minutes. Samples were centrifuged

at 5,000 x g for 10 minutes at 4 °C. The supernatant containing cytoplasmic proteins was discarded. Pellets were resuspended and washed with Buffer A and centrifuged again. After aspirating the supernatant, pellets were resuspended in 200 µL of Buffer B (20 mM HEPES pH 7.9, 25% glycerol, 420 mM NaCl, 1.2 mM MgCl₂, 0.2 mM EDTA, 0.5 mM DTT, 0.5 mM PMSF) and sonicated using a Sonic Dismembrator Model 100 (Fisher Scientific, Waltham, Massachusetts). Samples were incubated on ice for 30 minutes, then centrifuged at 16,000 x g for 30 minutes at 4 °C. Supernatant containing nuclear protein was collected. Nuclear protein was quantified using Lowry protein assay, and stored at -80 °C.

2.5.2 NF-κB ELISA

NF-κB (p65) relative binding activity was detected using an ELISA kit (Abcam, ab133112), according to the manufacturer's protocol. Briefly, nuclear protein samples were loaded to a plate, coated with a specific double stranded DNA sequence containing the NF-κB response element. As well, nonspecific binding buffer, positive control, and competitive inhibitor were each loaded to a well. NF-κB was specifically bound by the addition of a primary antibody. An HRP-conjugated secondary antibody was added, and the assay was read at 450 nm using a SpectraMax M5 (Molecular Devices, San Jose) and SoftMax Pro software.

2.6 Western Blotting

2.6.1 Protein lysis from LV tissues

Protein was extracted from left ventricular tissue from mice treated for 0.5 hour with LPS (4 mg/kg). Tissues were washed with cold PBS and minced mechanically in lysis buffer on ice using a tissue grinder. Samples were centrifuged at 5,000 x g at 4 °C for 5 minutes to separate tissue and cells from protein lysate. Protein concentration was quantified using Lowry assay, and the protein standard curve was extrapolated from bovine serum albumin (BSA) standards. Protein samples were read using a SpectraMax M5 (Molecular Devices, San Jose) and SoftMax Pro software. Loading protein samples were made for 75 µg protein/sample, diluted with lysis buffer.

2.6.2 Protein lysis from cardiomyocytes

Protein was lysed from cardiomyocyte cultures treated with LPS (5 µg/ml) for 0.5 hour. After washing cells with PBS, cells were mechanically disrupted with a pipette in lysis buffer and the lysate transferred into Eppendorf tubes. The lysate was then sonicated using a Sonic Dismembrator Model 100 (Fisher Scientific, Waltham, Massachusetts). Cells were separated from the protein lysate through centrifugation (5,000 x g at 4 °C for 5 minutes). Protein concentration was quantified using a Lowry assay, as described above.

2.6.3 Immunoblotting

Loading dye (4x: 0.125 M Tris-HCl pH 6.8, 20% glycerol, 0.4% SDS, 0.1% 2-mercaptoethanol, 0.1% bromophenol blue) was added to each sample, and samples were held for 5 minutes at 95°C. Seventy-five µg of protein was loaded onto an 8% SDS-polyacrylamide gel. The gel was run at 100 V for 2.5 hours. Then, proteins were wet transferred to a 0.45 µm polyvinylidene difluoride (PVDF) membrane at 100 V for 1 hour. The membrane was blocked in 5% skim milk for 1 hour at room temperature on a rotator. Then, the membrane was incubated with primary antibody overnight at 4°C, on a rotator. The membrane was washed with 0.1% Tween-20 tris-buffered saline (TBS-T) and then incubated with secondary antibody. The membrane was washed with TBS-T and visualized on film or by fluorescence on Odyssey (LI-COR Biosciences, Lincoln, Nebraska). For film visualization, a solution of part A (1:5) and part B (1:50) of automatic X-ray developer concentrate (White Mountain Imaging, Webster, New Hampshire) was used to develop the film in the dark. The signal was quantified by densitometry reading using FluorChem 8000. The dilution of primary and secondary antibodies used are shown in Table 2.2.

Table 2.2. Primary antibody concentrations and the corresponding secondary antibody concentrations used for immunoblotting.

Primary antibody	Secondary antibody
1:1000 Phospho-ERK1/2 (#9101, Cell Signaling Technologies, Danvers, MA)	1:1000 Goat anti-Rabbit Alexafluor 680 (#926-68021, LI-COR Biosciences, Lincoln, Nebraska)
1:1000 Total-ERK1/2 (#sc-94, Santa Cruz Biotechnology, Dallas, TX)	
1:1000 Phospho-p38 MAPK (#9211, Cell Signaling Technologies, Danvers, MA)	1:1000 Goat anti-Rabbit Alexafluor 680 (#926-68021, LI-COR Biosciences, Lincoln, Nebraska) OR; 1:1000 Goat anti-Rabbit-HRP (#170-6515, Bio-Rad, Hercules, California)
1:1000 Total-p38 MAPK (#9212, Cell Signaling Technologies, Danvers, MA)	
1:1000 α -actinin (#A7811, Sigma, St. Louis, MO)	1:1000 Goat anti-mouse-HRP (#170-6516, Bio-Rad, Hercules, California)

2.7 Echocardiography

Echocardiography was performed on WT and *RGS2^{-/-}* mice using the Vevo 2100 High-Resolution Imaging System (FUJIFILM VisualSonics, Toronto) for a non-invasive visualization of the left ventricle.

First, mice were pre-anaesthetized in a chamber, using 3.0% isoflurane gas. Fur was removed from the chest area using a small amount of hair-removal cream (Nair). Mice were quickly moved from the chamber and placed in the supine position on a heated electrode platform (temperature 37 °C) with their noses in a respirator used to deliver 0.5-1.5% isoflurane (for anesthesia maintenance). The mice were secured to the platform, with their paws over the electrode surface pads so that the electrocardiography (ECG) could be recorded. Electrode cream (Parker Labs, NJ, USA) was used to enhance the conductivity between their paws and the electrode pads. Pre-heated Aquasonic ultrasound transmission gel (Parker Labs, NJ, USA) was applied copiously on the chest over the heart, and the LV was visualized using the MS250S transducer probe (FUJIFILM VisualSonics). The heart was first visualized in the parasternal long axis view (PSLA). PSLA visualization was controlled by capturing the LV chamber at its widest diameter with a clear view of the aortic outflow and the apex. The probe was then turned 90° to visualize LV short-axis (SA). M-mode two-dimensional image captures were taken for each mouse. SA visualization was standardized among the mice by imaging the heart at the level where the papillary muscles could be detected. This also ensured the LV was imaged at the widest diameter. Each video/image capture was taken at a heart rate of 450-500 beats per minute (BPM) and body temperature around 37 °C, which allowed consistency between individual animals and was close to the awake physiological conditions of the mouse.

SA M-mode analysis was performed by marking the left ventricular anterior wall (LVAW), left ventricular internal dimension (LVID), and left ventricular posterior wall (LVPW) at both diastole and systole for three continuous heart cycles. Heart rate (HR) was determined from the continuous three heart cycles. Left ventricular ejection fraction (EF), fractional shortening (FS), LV anterior wall (AW) mass, and LV volume at systole and diastole (vol;s and vol;d) were calculated from SA M-mode analysis. Stroke volume (SV) was calculated

as the difference between LV;d and LV;s, and cardiac output (CO) was calculated as $CO = HR \times SV$. All measurements were performed on the Vevo 2100 Imaging System.

2.8 Statistical analysis

Data are presented as mean \pm standard error of the mean (SEM). Body weight and litter size were analysed using unpaired Student's t-test. Cardiac function parameters detected by echocardiography were analyzed using repeated measures two-way analysis of variance analysis (ANOVA), followed by Bonferroni's multiple comparisons test. All other data were analysed using two-way ANOVA followed by Tukey's *post-hoc* test. Statistical significance level was set at $\alpha = 0.05$. Grubbs test was used to detect for outliers, with $\alpha = 0.05$. Graphpad Prism (GraphPad Prism, version 5.0, CA, USA) was used for analysis and graphing of the results.

Chapter 3

3 Results

3.1 Body weight and litter size

WT and RGS2 deficient mice were used throughout *in vivo* experiments to assess the role of RGS2 in inflammatory cytokine release during endotoxemia. Male mice, 3-5 months old, were used. As well, P0 mice of both sexes were used for isolation of cardiomyocytes. RGS2 limits G α q- and G α s-coupled GPCR signaling and has been implicated in the cellular stress response.^{124,168} As it is ubiquitously expressed, we wanted to first assess the phenotype of *RGS2*^{-/-} mice. We found that *RGS2*^{-/-} mice had a lower average body weight than WT mice by 18.6% (Figure 3.1). We also found that *RGS2*^{-/-} mice had significantly smaller litters than WT mice (Figure 3.2, $P < 0.001$). These results are consistent with previous studies that showed lower body weight and smaller litter sizes in *RGS2*^{-/-} mice.^{169,170}

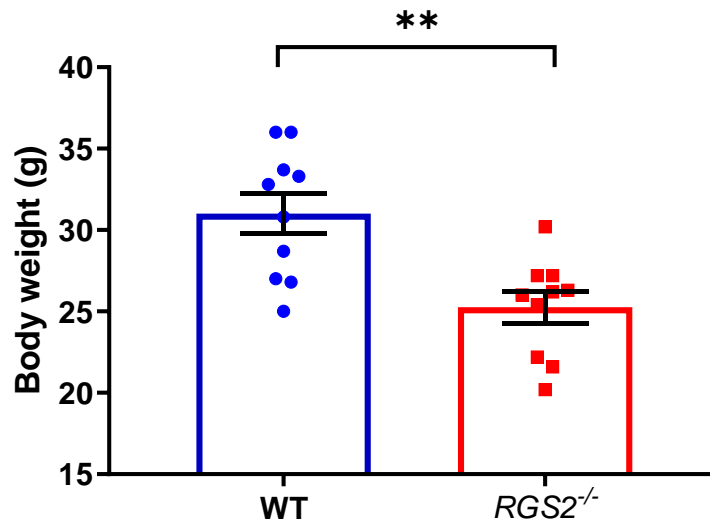


Figure 3.1. Body weight (g) of WT and *RGS2*^{-/-} mice. Mice used were 3-5 months old. Data are presented as individual values and their mean \pm SEM. $n = 10$ mice per group. ** $P < 0.01$ vs. WT.

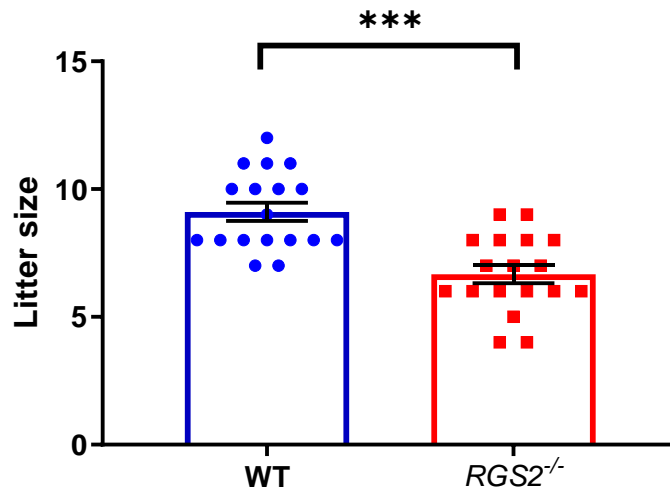


Figure 3.2: Litter sizes of WT and *RGS2*^{-/-} mice. Presented are individual values and average number of pups per litter \pm SEM. n = 18 per group. ****P*<0.001 vs. WT.

3.2 RGS2 mRNA levels in the heart during endotoxemia

RGS2 is implicated in many physiological and cellular processes, including blood pressure regulation and cardiac hypertrophy.^{135,136} To assess the effects of LPS stimulation on RGS2 expression, we analyzed RGS2 mRNA levels using qPCR. Previous studies investigating agonist stimulated RGS2 expression used time points from 0.5-12 hours.¹⁷¹ Specifically, in cardiomyocytes, RGS2 mRNA levels were analyzed after 0.5-3 hours of agonist treatment.^{155,172} Thus, we collected LV tissues from WT and *RGS2*^{-/-} mice 2 hours after LPS (4 mg/kg, IP) or saline control treatment. RNA was isolated and reverse transcribed to be analyzed by qPCR. We found that LPS stimulation *in vivo* did not affect RGS2 mRNA expression in the heart in WT mice (Figure 3.3). As expected, RGS2 deficient mice displayed negligible or no RGS2 mRNA content in the heart.

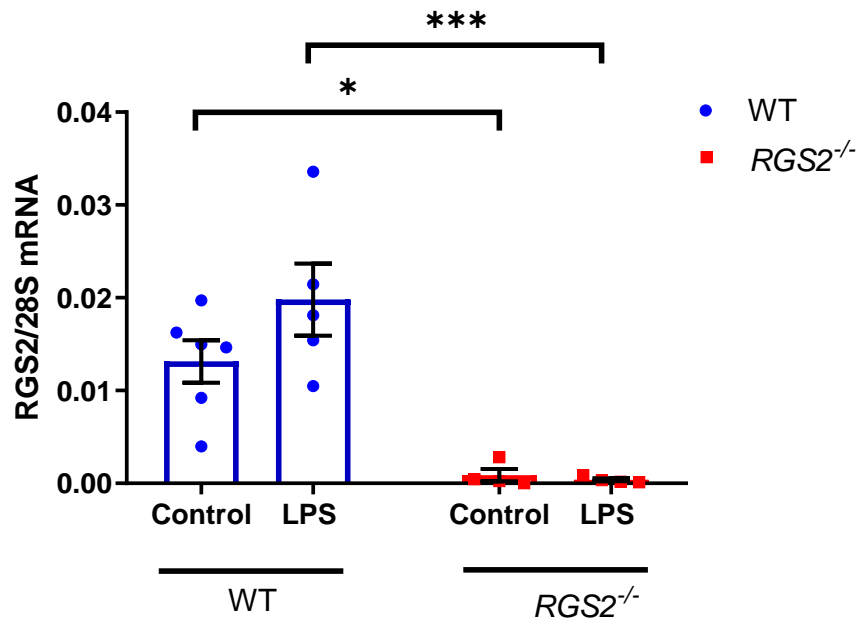


Figure 3.3. RGS2 mRNA level in WT LV after LPS treatment *in vivo*. Mice were treated hours with LPS (4 mg/kg, IP) or saline control for 2 hours. RNA was isolated from LV and reverse transcribed to cDNA. qPCR was performed and RGS2 mRNA levels were normalized to 28S using the standard curve method. Data are presented as individual values and their mean \pm SEM. n = 4-6 mice per group. * $P < 0.05$, ** $P < 0.01$ vs. respective WT.

3.3 TNF- α mRNA and protein levels in the heart after LPS treatment *in vivo*

To assess the role of RGS2 in inflammatory cytokine release during endotoxemia, the expression of TNF- α induced by LPS was assessed as an indicator of the inflammatory response. We treated WT and *RGS2*^{-/-} male mice with LPS (4 mg/kg, IP) or saline as control and collected plasma and LV tissues. To assess myocardial TNF- α mRNA levels, LV tissues were collected from mice 2 hours after LPS or control saline injection and qPCR analysis was performed.

LPS treatment for 2 hours in WT and *RGS2*^{-/-} mice showed higher TNF- α mRNA levels compared to their respective saline controls ($P < 0.01$). Notably, higher TNF- α mRNA levels were further enhanced in *RGS2*^{-/-} compared to WT mice ($P < 0.05$), which suggests that RGS2 has a regulatory role in proinflammatory cytokine release induced by LPS (Figure 3.4).

To assess the effects on TNF- α mRNA levels, WT and *RGS2*^{-/-} mice were injected with LPS (4 mg/kg, IP) and blood was collected via cardiac puncture at 0.5, 2, 4, or 24 hours after injection. Plasma was isolated via centrifugation. TNF- α was measured by an ELISA. There was no significant change in plasma TNF- α levels detected at 0.5 hours (Figure 3.5). In the WT samples, plasma TNF- α plateaued and started to decrease approximately 2 to 4 hours after LPS stimulation. Comparatively, in plasma of *RGS2*^{-/-} mice, TNF- α levels were significantly higher after 2 hours ($P < 0.05$) and continued to increase, as shown by the higher plasma TNF- α level at 4 hours ($P < 0.01$) of LPS treatment. At 24 hours post-LPS injection, plasma TNF- α levels of both WT and *RGS2*^{-/-} mice were comparable to control levels ($P > 0.05$ compared to 0 hour). We found the plasma TNF- α levels for WT mice to be consistent with previous studies from our lab.³³

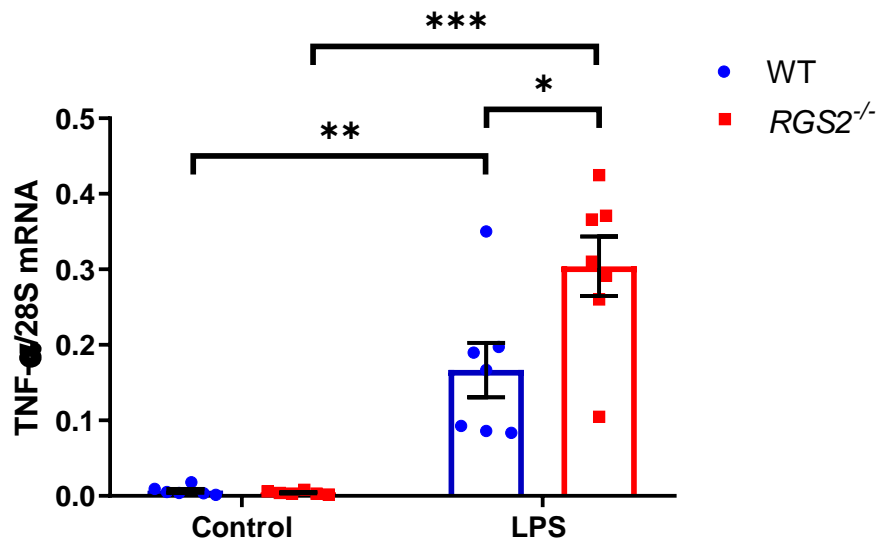


Figure 3.4. WT and *RGS2*^{-/-} LV TNF- α mRNA levels 2 hours after LPS treatment. Male mice were treated with LPS (4 mg/kg, IP) or saline control for 2 hours. RNA was isolated from LV and reverse transcribed to cDNA. qPCR was performed and TNF- α mRNA level was normalized to 28S using the standard curve method. Data are presented as individual values and their mean \pm SEM. $n = 7$ mice per group. * $P < 0.05$; ** $P < 0.01$; *** $P < 0.001$ vs. respective WT or control treatment.

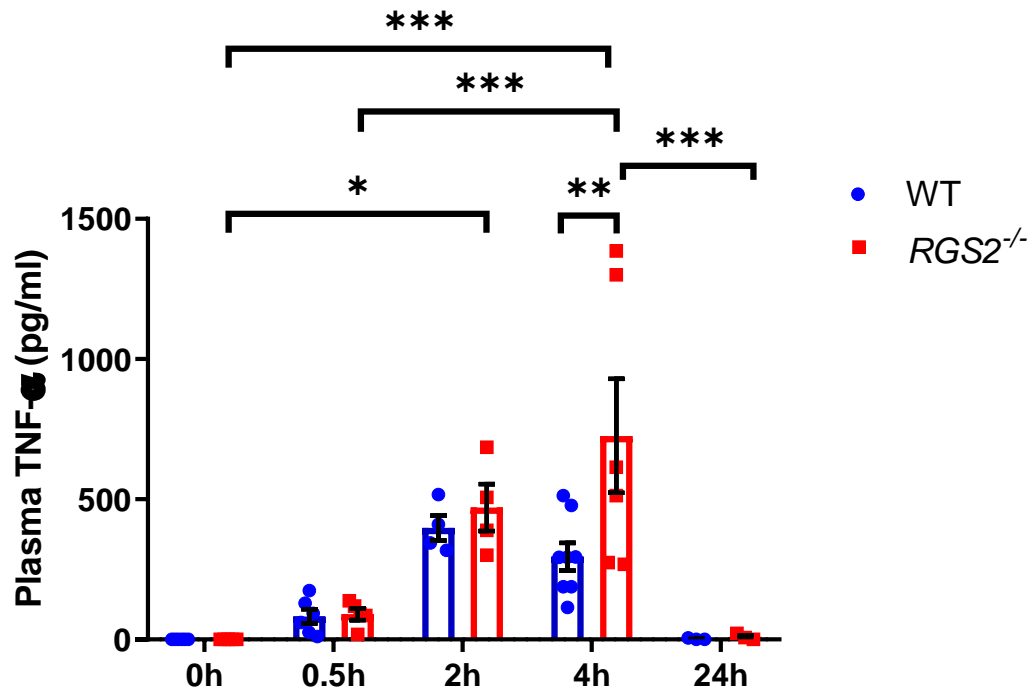


Figure 3.5. Plasma TNF- α levels in WT and *RGS2*^{-/-} during endotoxemia. Male mice were treated with LPS (4 mg/kg, IP) for 0.5, 2, 4, and 24 hours. Blood was collected via cardiac puncture and plasma was isolated by centrifugation. Plasma TNF- α protein levels were detected using an ELISA kit. Data are presented as individual values and their mean \pm SEM. n = 3-8 mice per group. * P <0.05, ** P <0.01, *** P <0.001 vs. respective WT or LPS stimulation.

3.4 TNF- α mRNA and protein levels in cardiomyocytes

To complement the *in vivo* model and further investigate the changes observed in Figures 3.4 and 3.5, neonatal cardiomyocytes were isolated from P0 WT and *RGS2*^{-/-} mice. This experiment would further clarify if the increases in TNF- α observed in the *in vivo* model might derive at least in part from cardiomyocytes. Again, the role of RGS2 in LPS-stimulated inflammatory cytokine release was assessed.

Cultured cardiomyocytes were treated with LPS (5 μ g/ml) or medium as control for 2 hours. RNA was isolated from the cardiomyocytes, and TNF- α mRNA levels were detected using qPCR. Similar to the *in vivo* results, LPS stimulated TNF- α mRNA expression in both WT and *RGS2*^{-/-} cardiomyocytes compared to controls (Figure 3.6a, $P < 0.05$). Notably, LPS-induced TNF- α mRNA levels were further enhanced in *RGS2*^{-/-} cardiomyocytes compared to WT (Figure 3.6**Error! Reference source not found.**a, $P < 0.01$).

To investigate changes in TNF- α release, WT and *RGS2*^{-/-} cardiomyocytes were treated with LPS (5 μ g/ml) or medium as control for 4 hours. Since global TNF- α release showed a significant difference between WT and *RGS2*^{-/-} mice at 4 hours (Figure 3.5), we chose this treatment period to evaluate any differences between cardiomyocytes isolated from the two genotypes. An ELISA kit was used to detect TNF- α release in the cell media. Similar to the *in vivo* results, higher TNF- α proteins were found to be released into the cardiomyocyte culture medium when treated with LPS compared to control. This effect again was exacerbated in the *RGS2*^{-/-} mice (Figure 3.6b, $P < 0.001$ and $P < 0.01$, respectively).

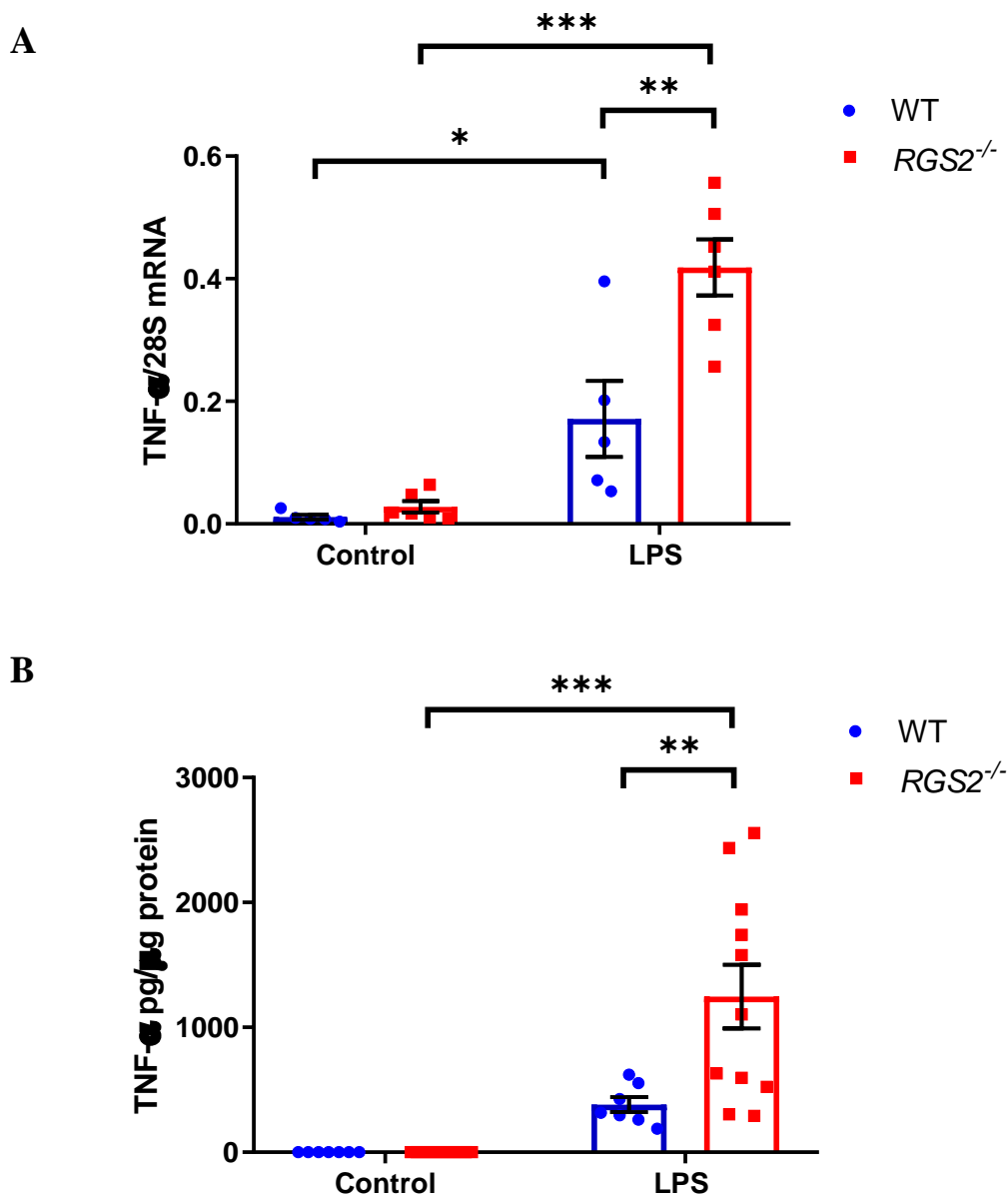


Figure 3.6. LPS-induced TNF- α levels in WT and *RGS2*^{-/-} cardiomyocytes. A) RT-qPCR analysis of TNF- α mRNA in WT and *RGS2*^{-/-} neonatal cardiomyocytes treated with LPS (5 μ g/ml) for 2 hours. n = 5-6 mice per group. B) Detection via an ELISA of TNF- α release using media collected from WT and *RGS2*^{-/-} cardiomyocyte cell cultures treated with LPS (5 μ g/ml) for 4 hours. TNF- α levels were normalized to total cell protein levels as determined by Lowry protein assay. Culture medium was used as control treatment. n = 7-11 mice per group. Data are presented as individual values and their mean \pm SEM. * P <0.05; ** P <0.01; *** P <0.001 vs. respective WT or control treatment.

3.5 Interleukin mRNA levels in the heart during endotoxemia

During septic conditions, proinflammatory cytokines are induced, including IL6 and IL-1 β . We wanted to assess if RGS2 has a central role in regulating the production of inflammatory cytokines other than TNF- α . IL-6 and IL-1 β have initial peak timepoints similar to TNF- α in endotoxemic mice, which suggests that an altered mRNA response of IL-6 and IL-1 β may be detectable at 2 hours post-LPS injection.¹⁷³ Thus, we analyzed the mRNA levels of these cytokines in LV tissues samples collected from WT and *RGS2*^{-/-} mice 2 hours after LPS (4 mg/kg, IP) treatment or saline control treatments.

Using qPCR analysis, LPS stimulated IL6 mRNA expression in both WT and *RGS2*^{-/-} mice (Figure 3.7, $P < 0.01$ and $P < 0.001$, respectively). However, no significant difference was found between WT and *RGS2*^{-/-} mice.

Similarly, IL-1 β mRNA levels were upregulated in the heart during endotoxemia in both WT and *RGS2*^{-/-} mice (Figure 3.8, $P < 0.01$ and $P < 0.001$, respectively). No significant difference was found between WT and *RGS2*^{-/-} mice when treated with LPS.

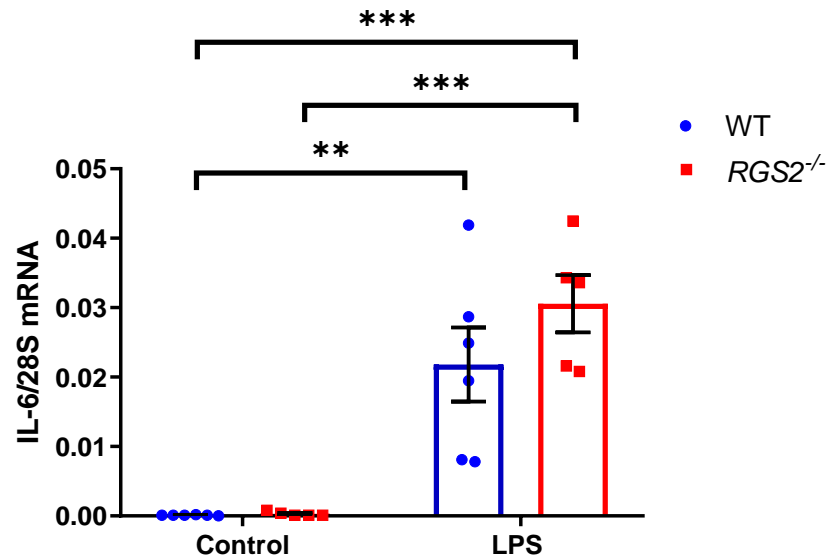


Figure 3.7. Myocardial IL-6 mRNA levels in WT and *RGS2*^{-/-} mice after LPS treatment *in vivo*. WT and *RGS2*^{-/-} male mice were treated with LPS (4 mg/kg, IP) or saline controls for 2 hours. RNA was isolated from LV and reverse transcribed to cDNA. qPCR analysis was performed, and IL-6 mRNA levels were normalized to 28S using the standard curve method. Data are presented as individual values and their mean ± SEM. n = 5-6 mice per group. ***P*<0.01, ****P*<0.001 vs. respective controls.

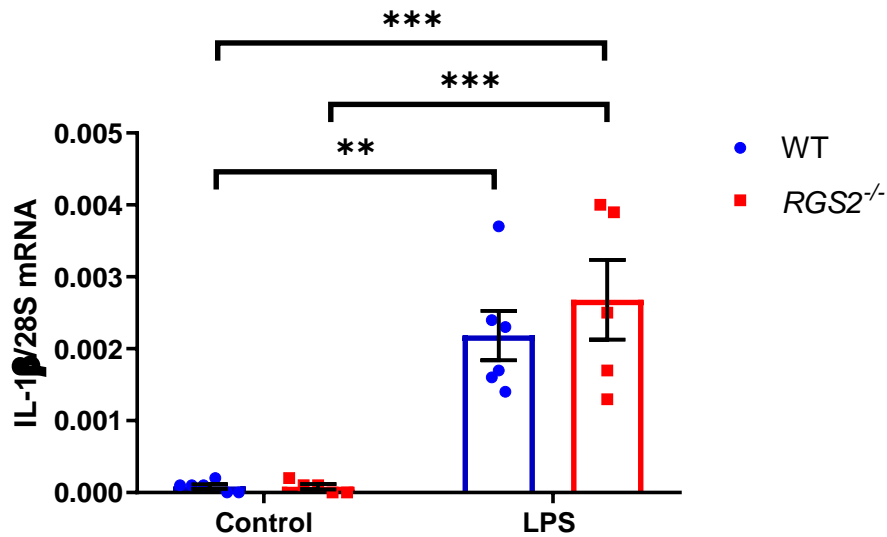


Figure 3.8. Myocardial IL-1 β mRNA levels in WT and *RGS2*^{-/-} mice after LPS treatment *in vivo*. WT and *RGS2*^{-/-} male mice were treated with LPS (4 mg/kg, IP) or saline controls for 2 hours. RNA was isolated from LV and reverse transcribed to cDNA. qPCR analysis was performed and IL-1 β mRNA levels were normalized to 28S using the standard curve method. Data are presented as individual values and their mean \pm SEM. n = 5-6 mice per group. ** P <0.01, *** P <0.001 vs. respective controls.

3.6 Left ventricular cardiac function in endotoxemia

The detrimental effect of LPS on cardiac function was previously shown to be mediated through the production of proinflammatory cytokines.²⁹ LPS-stimulated proinflammatory cytokine TNF- α has been suggested to be a main component in cardiac dysfunction.²⁵ Patients with sepsis often have impaired cardiac function, as a consequence of elevated proinflammatory cytokine levels.³⁰ To investigate whether RGS2 deficiency would exacerbate cardiac dysfunction, we performed echocardiography on WT and *RGS2*^{-/-} mice at baseline and 24 hours after LPS treatment (4 mg/kg, IP; Figure 3.9, **Error! Reference source not found.**).

Short-axis M-mode was used to assess cardiac parameters including ejection fraction, fractional shortening, and LV anterior wall (AW) mass. As well, LVAW, LV internal dimension (ID), and LV posterior wall (PW), each at end diastole (;d) and end systole (;s), were measured. Using short axis M-mode analysis, we found that LV ejection fractions of both WT and *RGS2*^{-/-} mice were impaired during endotoxemia (

Figure 3.10a, $P < 0.001$ and $P < 0.01$, respectively). At baseline, *RGS2*^{-/-} mice had a lower ejection fraction, which was further exacerbated by LPS treatment (

Figure 3.10a, $P < 0.01$ and $P < 0.05$, respectively). A similar trend was detected for LV fractional shortening, as shown in

Figure 3.10b. LPS treatment resulted in reduced fractional shortening in both WT and *RGS2*^{-/-} mice. Notably, LV fractional shortening associated with RGS2 deficiency weakened cardiac function under both basal and endotoxemic conditions ($P < 0.01$ and $P < 0.05$ respectively). Stroke volume was calculated as the difference between diastolic and systolic LV volume, and was significantly lower after LPS treatment in both WT and *RGS2*^{-/-} mice (Table 3.1, $P < 0.01$ and $P < 0.001$, respectively). Similarly, cardiac output was also lower after LPS treatment in WT and *RGS2*^{-/-} mice (Table 3.1, $P < 0.001$). There were no significant differences in stroke volume or cardiac output between WT and *RGS2*^{-/-} mice at baseline and LPS-treated conditions. Finally, no significant differences were found for heart rate and LV AW mass (Table 3.1, $P = \text{n.s.}$).

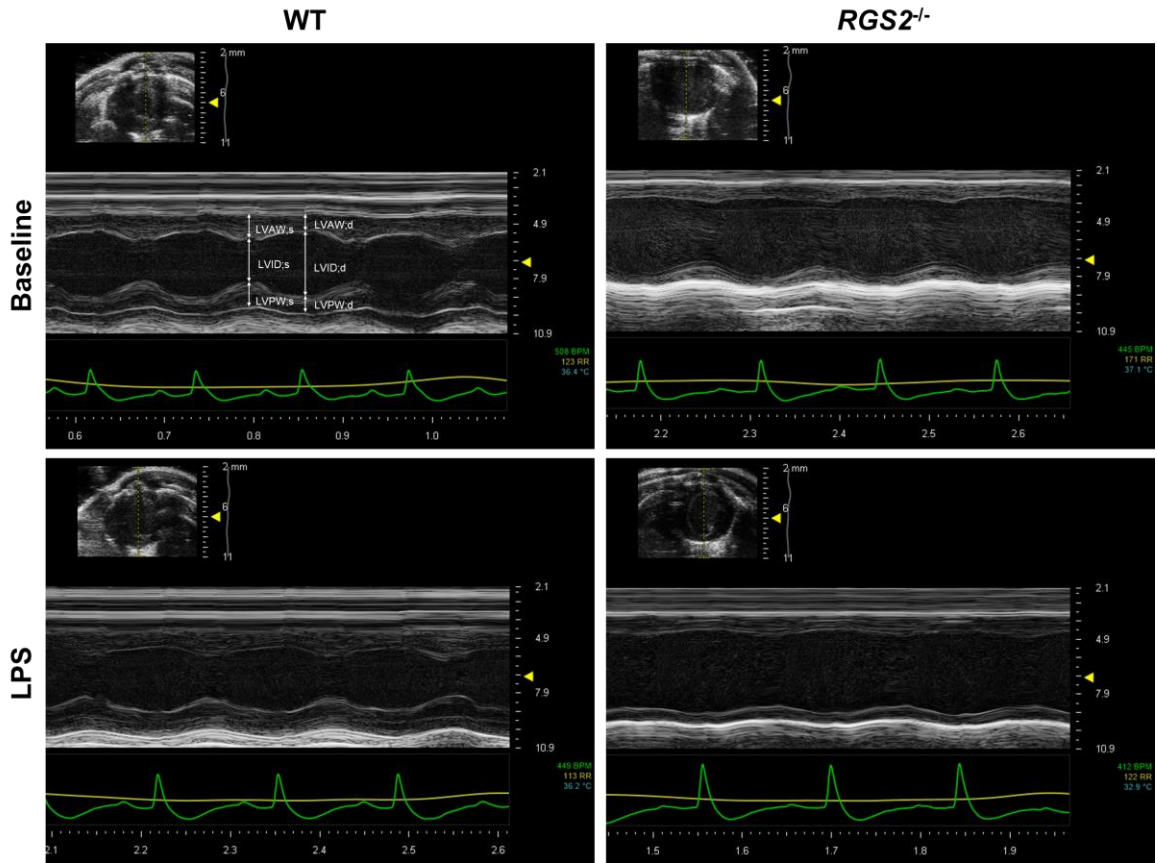


Figure 3.9. Representative short-axis and M-mode images of the left ventricle in WT and *RGS2*^{-/-} mice. Cardiac function in WT and *RGS2*^{-/-} mice was determined using echocardiography at baseline and 24 hours after LPS (4 mg/kg, IP) treatment. Shown are LV short axis images at the level of the papillary muscles. LVAW: left ventricular anterior wall; LVID: left ventricular internal dimension; LVPW: left ventricular posterior wall; d: end diastole; s: end systole.

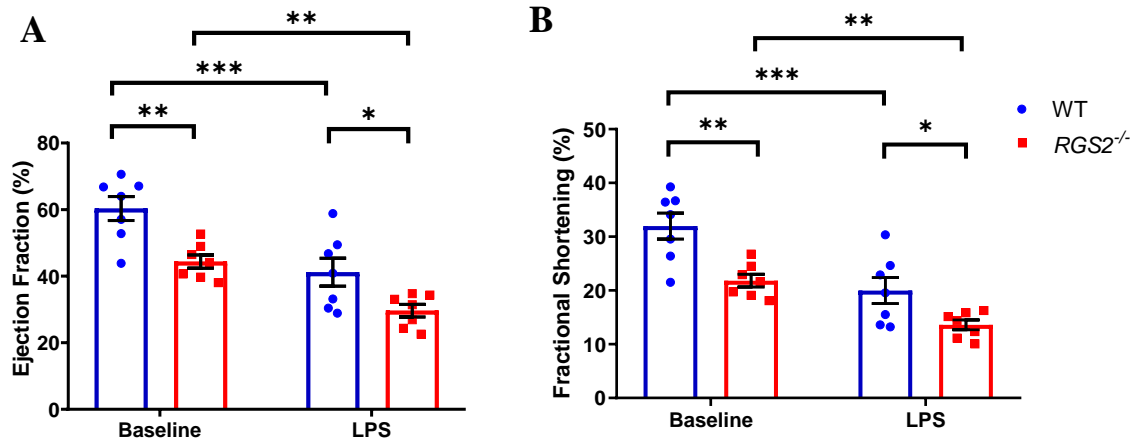


Figure 3.10. LV ejection fraction and fractional shortening in WT and *RGS2*^{-/-} mice. Echocardiography was performed in WT and *RGS2*^{-/-} mice at baseline and 24 hours after LPS (4 mg/kg, IP) treatment. n = 7 mice per group. A) Ejection fraction and B) fractional shortening were analyzed using LV short-axis M-mode. Data are presented as individual values and their mean ± SEM. **P*<0.05; ***P*<0.01; ****P*<0.001 vs. respective WT or baseline condition.

Table 3.1. Tabular summary of cardiac function in WT and *RGS2*^{-/-} mice analyzed by short-axis M-mode echocardiography.

Parameters	WT		<i>RGS2</i> ^{-/-}	
	n = 7		n = 7	
	Baseline	LPS	Baseline	LPS
Heart Rate (BPM)	463.9 ± 16.7	457.6 ± 17.8	435.8 ± 15.7	461.7 ± 12.6
Ejection Fraction (%)	60.3 ± 3.6	41.2 ± 4.2***	44.4 ± 2.0††	29.6 ± 1.9***†
Fractional Shortening (%)	32.0 ± 2.4	20.0 ± 2.4***	21.8 ± 1.2††	13.6 ± 0.9***†
Stroke Volume (μL)	39.4 ± 2.8	24.4 ± 2.8**	35.3 ± 1.6	17.9 ± 1.5***
Cardiac Output (mL/min)	18.2 ± 1.3	11.0 ± 1.3***	15.4 ± 1.0	8.2 ± 0.6***
LVAW;d (mm)	0.8 ± 0.0	0.8 ± 0.1	0.6 ± 0.0	0.9 ± 0.1*
LVAW;s (mm)	1.2 ± 0.1	1.0 ± 0.1	0.9 ± 0.0††	1.0 ± 0.1
LVID;d (mm)	3.9 ± 0.1	3.7 ± 0.2	4.2 ± 0.1	3.8 ± 0.2
LVID;s (mm)	2.7 ± 0.2	3.0 ± 0.2	3.3 ± 0.1††	3.3 ± 0.2
LVPW;d (mm)	0.7 ± 0.1	0.7 ± 0.1	0.6 ± 0.1	0.7 ± 0.1
LVPW;s (mm)	1.1 ± 0.1	0.9 ± 0.1	0.8 ± 0.1	0.8 ± 0.1
LV AW Mass (mg)	82.8 ± 7.2	74.4 ± 8.9	74.0 ± 4.8	82.8 ± 3.5

Echocardiography was performed in WT and *RGS2*^{-/-} mice at baseline and 24 hours after LPS (4 mg/kg, IP) treatment. Heart function was measured using short-axis M-mode analysis. n = 7 mice per group. LVAW: left ventricular anterior wall; LVID: left ventricular internal dimension; LVPW: left ventricular posterior wall; d: end diastole; s: end systole. *P<0.05, **P<0.01, ***P<0.001 vs respective baseline condition. †P<0.05, ††P<0.01 vs. respective WT

3.7 MAPK phosphorylation levels in the heart

Previous studies from our lab showed MAPKs to be mediators in LPS-induced TNF- α production in the heart.^{26,61,62,65} ERK1/2 was suggested to have a role in the regulation of inflammatory cytokine expression.⁶⁶ Additionally, p38 MAPK α isoform is targeted by endotoxins in mammalian cells and regulates inflammatory cytokine release.^{67,68} We wanted to first confirm that ERK1/2 and p38 are involved in LPS-stimulated inflammatory cytokine release pathway. Since changes in MAPK activation occur relatively quickly after LPS stimulation, we extracted protein from LV tissues collected 30 minutes after LPS (4 mg/kg, IP) or saline control treatment.³³ We used immunoblotting to detect phosphorylated relative to total protein levels to assess MAPK activity.

ERK1/2 activity regulates LPS-stimulated TNF- α expression in cardiomyocytes.⁶⁵ This study found the ratio of phosphorylated to total ERK1/2 protein signals was higher in LPS-treated WT mice compared to control (Figure 3.11 **Error! Reference source not found.**, $P < 0.05$). Further, there were no significant difference in phosphorylated ERK1/2 levels at baseline or after LPS treatment between WT and *RGS2*^{-/-} mice (Figure 3.11, $P = \text{n.s.}$).

Similarly, p38 signaling is enhanced during sepsis, and induces TNF- α production in the heart.³³ Previously, p38 inhibition was shown to alleviate myocardial depression in endotoxemia.³³ We found that while the ratio of phosphorylated to total p38 protein levels was not significantly higher in LPS-treated WT mice (Figure 3.12, $P = \text{n.s.}$), *RGS2*^{-/-} mice had significantly higher phosphorylated p38 levels than WT during endotoxemia (Figure 3.12, $P < 0.05$). These results suggest that p38 mediates the inflammatory response, and it is regulated by upstream RGS2 activity.

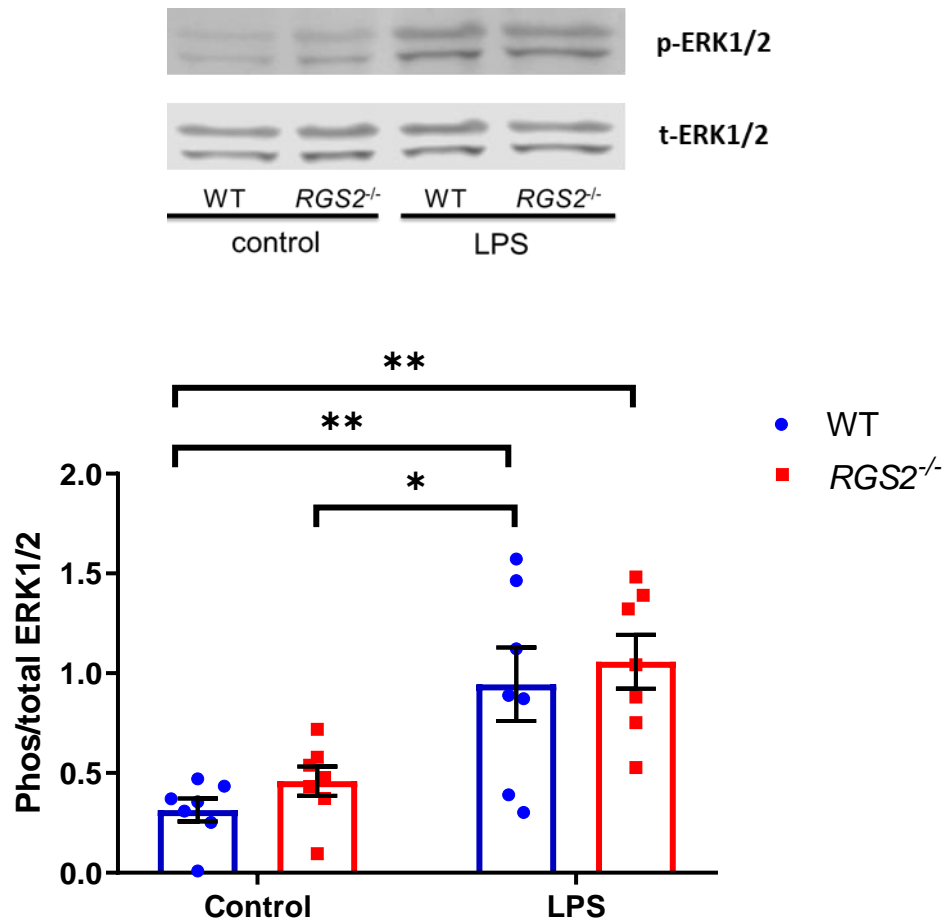


Figure 3.11. Myocardial ERK1/2 phosphorylation after LPS treatment *in vivo*. WT and *RGS2*^{-/-} mice were treated with LPS (4 mg/kg, IP) or saline control for 0.5 hr. Protein was extracted from LV. Western blot was performed to detect phosphorylated and total ERK1/2 protein levels. Data are presented as individual values and their mean ± SEM. N = 6 mice per group. **P*<0.05 vs. respective controls.

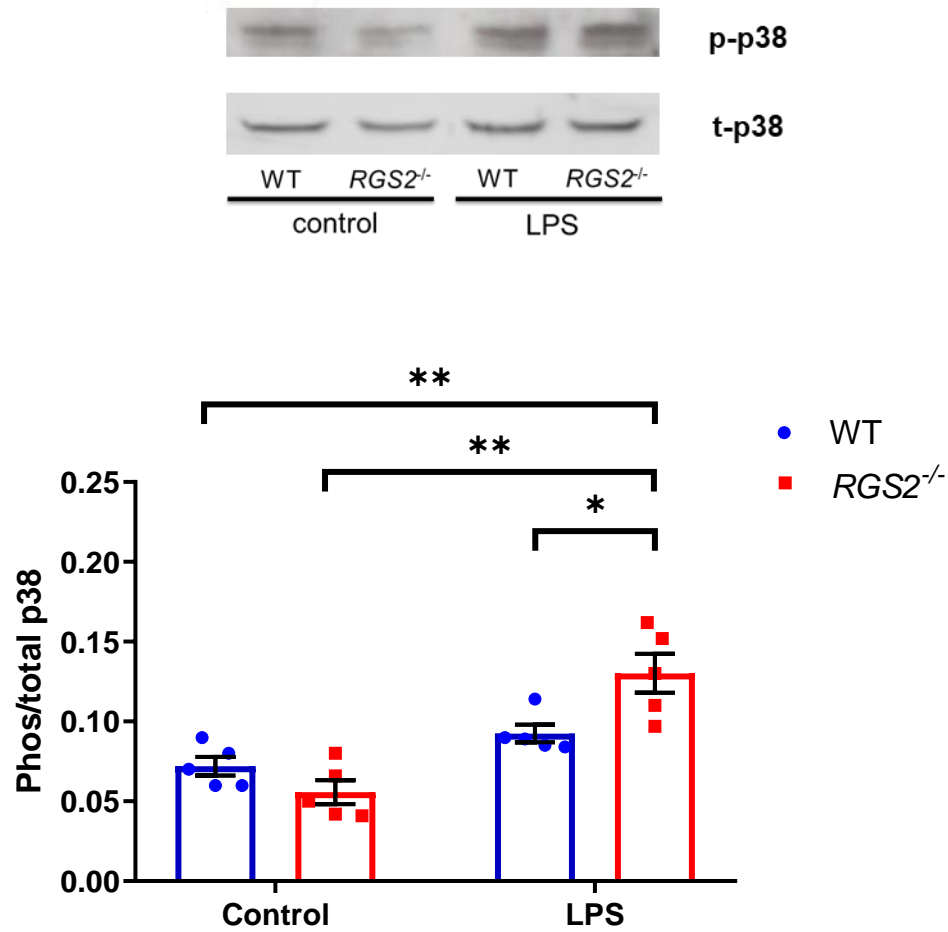


Figure 3.12. Myocardial p38 MAPK phosphorylation after LPS treatment *in vivo*. WT and RGS2^{-/-} male mice were treated with LPS (4 mg/kg, IP) or saline control for 0.5 hr. Protein was extracted from LV. Western blot was performed to detect phosphorylated and total p38 protein levels. Data are presented as individual values and their mean ± SEM. n = 5 mice per group. *P<0.05; **P<0.01 vs. respective WT or control treatment.

3.8 PKA-inhibition in cardiomyocytes

MAPK activity can be modulated through its phosphorylation state. PKA is a kinase upstream of MAPKs that has a role in regulating the activity of p38 and JNK.⁵⁸ PKA is also downstream of G protein signaling, and its activity can be induced by $G_{\alpha s}$, decreased by $G_{\alpha i}$, and unaffected by $G_{\alpha q}$ signaling.⁷⁰ This may be one of the ways that RGS2 modulates TLR4 signaling during endotoxemia. While p38 can be modulated by many upstream factors, including $G_{\alpha q}$ -PLC β -PKC activity, we were interested in investigating PKA as an inflammatory mediator since it has been shown to be involved in $G_{\alpha s}$ -stimulation of p38 signaling in cardiomyocytes.⁹⁶ In addition to regulating MAPK activity, PKA is a central regulator in many biochemical pathways and may affect TNF- α expression through other signaling factors.¹⁷⁴ To investigate its role, we used the PKA inhibitor H89 to pre-treat cardiomyocytes prior to LPS stimulation.

TNF- α mRNA levels were significantly higher in LPS treated *RGS2*^{-/-} cardiomyocytes (Figure 3.13, $P < 0.001$). With H89 pretreatment to inhibit PKA, LPS-stimulated TNF- α mRNA levels were significantly lowered in *RGS2*^{-/-} cardiomyocytes. There was no significant difference in TNF- α mRNA levels between DMSO+LPS and H89+LPS treatments in WT cardiomyocytes.

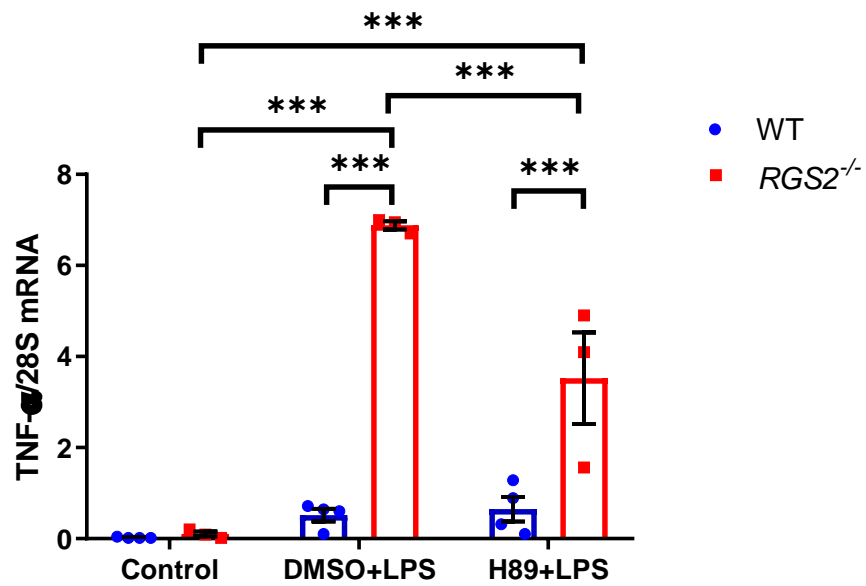


Figure 3.13. TNF- α mRNA levels in WT and *RGS2*^{-/-} cardiomyocytes after PKA inhibition. WT and *RGS2*^{-/-} cultures were pretreated with DMSO or H89 (20 μ M) for 0.5 hr, followed by LPS (5 μ g/ml) stimulation for 2 hours. RNA was isolated from cardiomyocytes and reverse transcribed to cDNA. qPCR was performed and TNF- α mRNA levels were normalized to 28S using the standard curve method. Data are presented as individual values and their mean \pm SEM. n = 3-4 mice per group. *** P <0.001 vs. respective WT, control, or LPS stimulation.

3.9 Relative NF- κ B activity in the heart

Upon LPS stimulation, the TLR4 signaling cascade activates transcription factors such as NF- κ B and the production of proinflammatory cytokines downstream.¹⁹ We wanted to confirm the role of NF- κ B in enhancing inflammatory cytokine release in the heart, and its involvement as a crosstalk mechanism. PKC has been shown to be upstream of the IKK complex, and thus may be able to modulate NF- κ B activity.¹⁵⁹ As well, PKC activity can be induced by upstream G α q-PLC β signaling. Thus, PKC can be modulated by RGS2 activity through the latter's regulation of G α q. To investigate NF- κ B activity in the heart, we isolated nuclear proteins from LVs collected 0.5 hours after LPS (4 mg/kg, IP) or saline control treatment. An ELISA kit was used to detect the presence of p65, a protein associated in NF- κ B heterodimer formation, nuclear translocation, and activation, in the nuclear protein samples.

In endotoxemia, a relatively higher level of NF- κ B activity was detected in WT mice (Figure 3.14, $P < 0.05$). *RGS2*^{-/-} mice showed a trend towards higher NF- κ B activity during endotoxemia, but no significant difference was found. Finally, no statistically significant differences were found between WT and *RGS2*^{-/-} LV myocardium ($P = \text{n.s.}$).

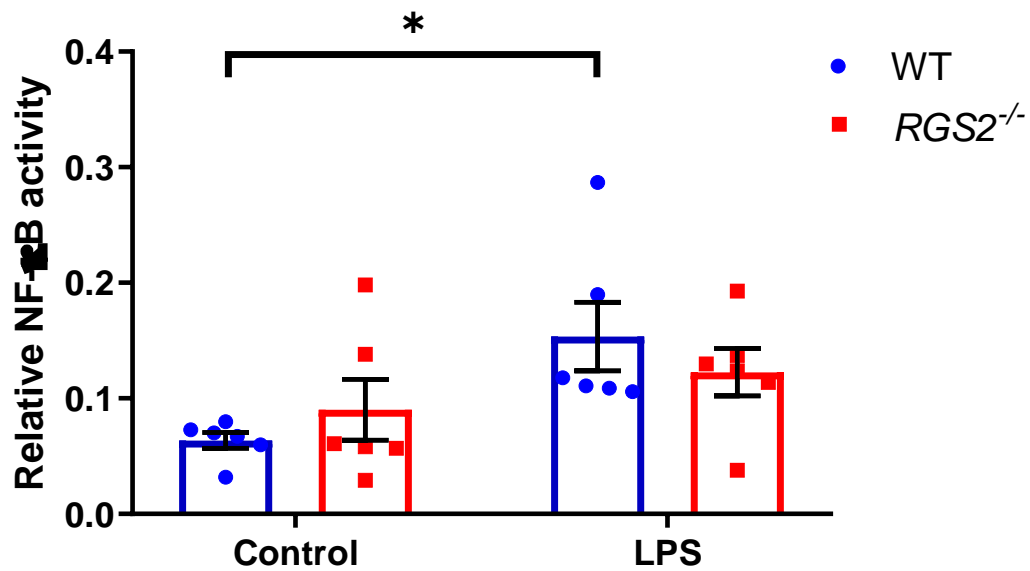


Figure 3.14. Relative NF-κB activity in WT and *RGS2*^{-/-} myocardium during endotoxemia. WT and *RGS2*^{-/-} mice were treated IP for 0.5 hour with LPS (4 mg/kg, IP) or saline control. Nuclear protein was extracted from LV and used for ELISA to detect relative NF-κB activity. Data are presented as individual values and their mean ± SEM, n = 6 mice per group. **P*<0.05 vs. WT control.

Chapter 4

4 Discussion

4.1 Summary

The present study, to our knowledge, is the first to investigate the role of RGS2 in the heart during endotoxemia. Our study shows that RGS2 deficiency enhances TNF- α proinflammatory response to LPS stimulation. During endotoxemia, plasma TNF- α levels were higher in WT mice and higher still in RGS2 deficient mice. Similarly, when assessing left ventricular TNF- α mRNA levels, we found that *RGS2*^{-/-} mice had higher levels during endotoxemia compared to WT mice. This exacerbation of the inflammatory response was reflected in cultured cardiomyocytes. With LPS treatment, cardiomyocytes showed higher TNF- α release and mRNA levels compared to untreated conditions. As well, when treated with LPS, *RGS2*^{-/-} cardiomyocytes were found to have higher TNF- α release and mRNA levels than WT cells. RGS2 regulates G protein signaling through GAP-dependent and -independent mechanisms. As well, it modulates protein synthesis, independent of its G protein regulation. This study also investigated possible pathways through which RGS2 affects inflammatory cytokine release during endotoxemia. Previously, we found that p38 is involved in the LPS-TLR4 pathway. This study demonstrated higher LPS-induced p38 phosphorylation in *RGS2*^{-/-} compared to WT hearts. Finally, this study demonstrated an exacerbated LV cardiac dysfunction during endotoxemia in *RGS2*^{-/-} mice. Collectively, these findings suggest that RGS2 may have a cardioprotective role in endotoxemia by modulating G protein signaling and downstream MAPK activity.

4.2 RGS2 deficiency affects body weight and litter size

RGS2 is expressed in the body globally and is involved in multiple cellular response pathways.^{168,170,175} Characteristics of RGS2 deficient mice have been demonstrated in past studies. Consistent with previous studies, we found that *RGS2*^{-/-} mice had lower body weights compared to WT mice when measured at 3 to 5 months of age.¹⁶⁹ This weight difference did not affect *RGS2*^{-/-} mice from reaching a healthy adult mouse weight.¹⁶⁹ RGS2 is involved in adipocyte differentiation and highly expressed in brown adipose

tissue.^{175,176} As a result, adipogenesis and function of white adipose tissue and brown adipose tissue may be weakened in RGS2 deficient mice.^{169,175}

In addition to lower body weight, it was interesting to note that *RGS2*^{-/-} mice produced smaller litter sizes. This is consistent with previous reports of the role of RGS2 in reproduction – namely, it helps maintain mouse egg fertilization by suppressing premature Ca²⁺ release.¹⁷⁰ While the role of RGS2 in the heart during sepsis has not been studied, a recent study showed that RGS2 has a bronchoprotective role in LPS induced airway inflammation.¹⁷⁷ However, no clear anti-inflammatory effect was detected as there was no significant difference found in proinflammatory levels between WT and *RGS2*^{-/-} mice.¹⁷⁷ Other RGS proteins have been implicated in the inflammatory response, including RGS1, RGS4, RGS10, and RGS16.^{178–182} In periodontal tissue, RGS10 knockdown reduced local proinflammatory cytokine expression.¹⁸¹ RGS10 also regulates TNF- α levels in ovarian cancer cells through a G α i-independent mechanism.¹⁸⁰ Similarly, RGS16 knockdown enhances proinflammatory cytokine expression, and overexpression reduces the inflammatory response in monocytes.¹⁷⁹ In sepsis, RGS4 and RGS16 levels were enhanced in the heart corresponding with decreased PLC activity.¹⁸² Similarly, Panetta *et al.* found RGS1 and RGS16 to be upregulated in the heart and aorta of septic animals, suggesting a role in amplifying sepsis-mediated signaling pathways.¹⁷⁸ However, the role of RGS2 in the heart in sepsis is not clear.

4.3 RGS2 deficiency enhances the TNF- α proinflammatory response during endotoxemia

To investigate the role of RGS2 in inflammatory cytokine release during endotoxemia, we wanted to first examine if LPS stimulation changes RGS2 expression in the heart using qPCR analysis. Predictably, RGS2 mRNA was barely detected in *RGS2*^{-/-} mice. Further, there was no significant difference in RGS2 mRNA expression in the heart of WT mice with or without endotoxemia. However, our assessment of RGS2 mRNA at 2 hours may be a false negative result, given that previous studies have indicated RGS2 is an early gene that is upregulated immediately and transiently. This was demonstrated by Grant *et al.*, showing RGS2 mRNA upregulation by Ang II peaks at around 1 hour, so it could be possible that our results only assessed RGS2 expression during the downward phase.¹⁸³

While no studies to date have shown endotoxemia affects RGS2 mRNA expression in the heart, studies have shown that RGS2 expression is downregulated in murine macrophages after LPS treatment.^{184,185} LPS was also shown to affect the expression of other RGS proteins: RGS1 and RGS16 were upregulated in dendritic cells, RGS14 and RGS18 expression decreased in dendritic cells, RGS1 showed a biphasic response in macrophages, and RGS4 and RGS16 expression transiently increased in cardiomyocytes.^{182,184,186} This suggests that RGS2 levels are regulated depending on cell type, and our results indicate that RGS2 mRNA expression in the heart is not affected by LPS stimulation. Additionally, RGS2 protein levels increased after digoxin treatment while mRNA levels were not altered, due to inhibition of RGS2 protein degradation.¹⁵⁷ While we tried to detect relative RGS2 protein content in the heart of WT and *RGS2*^{-/-} mice, the immunoblot analysis did not work as we could not visualize the RGS2 antibody (not shown). Future experiments are required to assess RGS2 protein levels in the heart.

In our study, the time course of plasma TNF- α levels was studied after LPS injection, showing the highest plasma TNF- α levels at 2 hours in WT mice, which was consistent with previous studies.¹⁷³ In comparison, plasma TNF- α levels were significantly higher 2 and 4 hours after LPS treatment in *RGS2*^{-/-} mice. Thus, global TNF- α levels are higher in endotoxemia in *RGS2*^{-/-} mice, suggesting that RGS2 may have a regulatory role in proinflammatory response. This effect may be specific to an LPS-induced TNF- α response or possibly bacterial infection as loss of RGS2 impacts T-cell proliferation and reduces IL-2 levels in response to a viral infection.¹⁶²

TNF- α expression contributes to cardiovascular dysfunction in sepsis.^{33,71} Accordingly, TNF- α mRNA expression was analyzed in the heart of mice in the present study. Similar to changes in plasma TNF- α levels, we detected higher TNF- α mRNA expression in the LV tissues of *RGS2*^{-/-} mice compared to WT during endotoxemia. This novel finding is in sharp contrast with a recent study showing that LPS-induced TNF- α expression in bronchoalveolar lavage fluid was not significantly different between *RGS2*^{-/-} and WT mice.¹⁷⁷ This may suggest that while RGS2 is present in various tissues, its role during endotoxemia may differ depending on the tissue type.^{129,133,177}

To complement our *in vivo* study, experiments were carried out in primary neonatal cardiomyocytes. Consistent with our previous studies,³³ LPS induced TNF- α expression in WT cardiomyocytes. Notably, a significantly higher LPS-induced TNF- α production was found in *RGS2*^{-/-} compared to WT cardiomyocytes. The results show that RGS2 inhibits LPS-induced inflammatory response in cardiomyocytes.

4.4 Interleukin release is not affected by RGS2 deficiency

Exacerbated proinflammatory cytokine release is associated with the dysregulated immune response in sepsis. In addition to TNF- α , other inflammatory cytokines involved in the septic response include interleukins, such as IL-1 β and IL-6. Both interleukins were shown to be involved in sepsis, in both animal models and human studies.^{37,187} In the current study, WT mice also had significantly higher interleukin levels in endotoxemia. However, for both IL-1 β and IL-6, no significant difference was found between WT and *RGS2*^{-/-} mice during endotoxemia. One reason that interleukin levels were not significantly different between the two genotypes is possibly because peak mRNA levels for the interleukins may occur at around 4-6 hours after LPS injection,³⁷ which could be assessed in future studies. As well, while interleukins act synergistically with TNF- α during sepsis, they are activated through a different pathway than that of TNF- α . As well, the lack of significant difference in myocardial interleukin levels between WT and *RGS2*^{-/-} mice may be due to different autocrine and paracrine signaling pathways of TNF- α , IL1 β , and IL-6. For example, in human astrocytoma cells, PKC and reactive oxygen intermediates (ROIs) were involved in IL-6 and TNF- α gene expression induced by IL-1 β . However, protein tyrosine kinases only aided in IL-6 expression.¹⁸⁸ The present study suggests that IL-1 β and IL-6 expression are not regulated by RGS2 in the heart during endotoxemia.

4.5 Cardiac dysfunction is exacerbated in *RGS2* deficient mice

Cardiac dysfunction is associated with inflammation in a feedforward manner.^{189,190} As part of this detrimental loop, peripheral tissues release inflammatory signaling molecules that mediate the progression of heart failure. Long term exposure to inflammatory cytokines also exacerbates myocardial damage and enhanced proinflammatory expression

are indicators of mortality in severe heart failure patients.^{189,191} As part of the feedforward cycle, heart failure further stimulates inflammation in cardiac cells. This is activated by stress signals in the damaged cells, which cause further inflammatory responses in peripheral tissues, including adipose tissue, spleen, and bone marrow.¹⁹⁰ Because of this harmful loop, understanding the pathophysiology is beneficial in order to regulate the early immune response to avoid sepsis and heart failure. Using echocardiographic imaging followed by M-mode analysis, we found that cardiac function was impaired during endotoxemia with decreased ejection fraction, fractional shortening, cardiac output, and stroke volume in both WT and *RGS2*^{-/-} mice. Heart rate was not significantly different between the treatments, which suggests that the impaired cardiac function is not due to varying heart rates. Notably, LV ejection fraction, and fractional shortening, were lower further in *RGS2*^{-/-} mice compared to WT at baseline and during endotoxemia. Our results show that RGS2 has an important role in maintaining cardiac function during endotoxemia.

In contrast to our data, a past study using *RGS2*^{-/-} mice showed no differences in cardiac function under basal conditions; however, they also showed a cardioprotective role of RGS2.¹⁵² This discrepancy may be because we performed echocardiography on anesthetized mice compared to conscious mice. Awake mice may undergo high stress conditions when echocardiography is performed, which could interfere with the cardiac function measurement. As well, there was a difference in the equipment used – our transducer allowed for clearer imaging of the heart, comparatively. Future experiments can investigate cardiac function using myocardial strain analysis, which is an even more sensitive method that has been proposed as a measure of monitoring cardiac function in sepsis mouse models.¹⁹²

4.6 p38 may be involved in a crosstalk mechanism

This study investigated the specific signaling mediators by which RGS2 regulates the inflammatory response in sepsis. MAPKs are signaling mediators critical to LPS-induced TNF- α production, and MAPK activity is induced in the heart during sepsis.^{26,61–63} Specifically, ERK1/2 and p38 MAPKs modulate TNF- α expression in cardiomyocytes, and function as positive regulators of the proinflammatory cytokine release.^{33,61,65} Similarly, our study found that LPS induces ERK1/2 and p38 phosphorylation in the LV myocardium.

RGS2 deficiency did not affect ERK1/2 phosphorylation in endotoxemia. In contrast, LPS-induced p38 phosphorylation was enhanced in *RGS2*^{-/-} mice. Previous studies have shown that inhibiting p38 signaling decreases myocardial TNF- α expression and improves cardiac function during endotoxemia.^{33,58}

While our study did not show ERK1/2 phosphorylation to be affected by RGS2, a previous study indicated that RGS2 overexpression suppresses oxytocin-stimulated activation of ERK1/2 and RGS2 silencing resulted in increased signaling via ERK1/2.¹⁹³ While ERK1/2 and p38 are parallel signaling MAPKs and are often found to function in tandem, they are also involved in many broad physiological processes. ERK1/2 and p38 are involved in crosstalk processes that may affect their individual phosphorylation. For example, increased expression of JNK/c-fos resulted in lower phosphorylation of ERK1/2 and p38, which leads to lower TNF- α expression in LPS-stimulated cardiomyocytes.⁶¹ Additionally, p38 is mainly regulated by *G α s* and *G α q*-signaling, but not *G α i*, whereas ERK1/2 can be regulated by *G α i*.⁷⁰ Since RGS2 has a low affinity for *G α i*, that may be another reason why ERK1/2 activity is not affected by RGS2 deficiency. RGS2 also functions on the level of G protein signaling, and MAPK activity can be affected by mediators other than RGS2. While our study may suggest that p38 and ERK1/2 are regulated differently by RGS2 during endotoxemia, future studies should investigate the MAPK phosphorylation levels in primary neonatal cardiomyocytes in addition to LV tissues.

To investigate how RGS2 modulates p38 activity, this study assessed the role of PKA, which is an upstream kinase that can phosphorylate MAPKs.⁵⁸ This study did not detect any significant differences in TNF- α mRNA levels when PKA was inhibited in WT cardiomyocytes. We found that PKA inhibition with LPS treatment resulted in lower TNF- α expression in *RGS2*^{-/-} cardiomyocytes. However, because our experiment had a small sample size, we cannot draw any conclusion on whether PKA is involved in RGS2's inflammatory regulation. Our results may also be due to PKA's broad role in many cellular processes, including apoptosis and myocardial dysfunction.^{58,115} As well, p38 can be activated by many mediators other than PKA, such as *G α q*-PLC β signaling.⁵⁸ Thus inhibiting PKA alone may not be enough to determine the role of RGS2 in regulating p38 in endotoxemia.

Finally, we assessed if RGS2 modulates NF- κ B activity induced by LPS. NF- κ B is a central mediator of proinflammatory cytokine expression and can prolong inflammatory conditions through a feed-forward loop via IKK activity.^{77,82} IKK complex function can be regulated by RGS2-mediated PKC.¹⁵⁹ Our study showed that LPS induces NF- κ B activation in the heart of WT mice during endotoxemia. This echoes previous papers that indicate LPS activation of TLR4 induces NF- κ B translocation.⁷⁵ We did not detect any difference in NF- κ B activity between *RGS2*^{-/-} and WT mice, suggesting that RGS2 may not regulate NF- κ B activity. The lack of significance may be due to the large variability within the *RGS2*^{-/-} group, and future experiments should aim to reduce the effect of variation by increasing sample size. Additionally, NF- κ B can be induced by numerous signaling factors.⁷⁷ Specifically, *G α s* signaling and *G α q* signaling have conflicting effects on NF- κ B activity – *G α s*-cAMP-PKA activity inhibits NF- κ B, whereas the $\beta\gamma$ -subunit and *G α q* induces NF- κ B.¹⁹⁴ Thus, it may be hard to determine the exact effect of RGS2 on NF- κ B without inhibiting or stimulating either *G α s* or *G α q* signaling. Presently, our study indicates that NF- κ B is not regulated by RGS2 during endotoxemia.

4.7 Limitations and future directions

Confines to the present study design include using globally knocked-out RGS2 mice to investigate inflammatory response in septic conditions in the heart. While we will isolate the effects in cardiomyocytes by using an *in vitro* model, it may be prudent to follow up the study using cardiomyocyte-specific *RGS2* knockout mice. As well, LPS treatment is used to model sepsis; however, endotoxemia conditions does not accurately reflect full clinical sepsis as it is only a component of Gram-negative bacteria and not live bacteria. Furthermore, only a third of septic cases were found to have originated from Gram-negative bacterial infections.³ Mice have been shown to be less sensitive to LPS than humans, even in more sensitive strains, and expresses varied endotoxemia gene profiles.²⁰ Thus, while our LPS model is sufficient for investigating the pathophysiology of sepsis, follow-up studies using other sepsis models (*e.g.* cecal ligation puncture, pneumonia-induced) may help enhance the clinical applicability of the results.²⁰ This study can also be replicated using human cells (*e.g.* human induced pluripotent stem cell derived cardiomyocytes) to confirm that cell signalling pathways and inflammatory response are

similar between species. This can be verified by investigating the proteomic expression of the environment in mouse and human cells.

While the current study looked at the overall role of RGS2 in the inflammatory response, future experiments can assess the involvement of each distinct RGS2 function. For example, we can determine whether RGS2 regulates proinflammatory cytokine production mainly via *G α s*, *G α q*, or eIF2B mechanism. This would also clarify how RGS2 modulates downstream mediators such as NF- κ B, which is regulated differently by both *G α s* and *G α q* signaling.¹⁹⁴ Additionally, future experiments may investigate whether mortality and the LD50 of LPS is impacted by RGS2 deficiency. Finally, since RGS2 is highly expressed in the immune system, a follow-up study may examine the contribution of RGS2 to pathogenic changes in sepsis.

4.8 Conclusions

To our knowledge, the present study is the first to show that RGS2 limits inflammatory cytokine expression in endotoxemia. In response to LPS, *RGS2*^{-/-} mice have higher plasma and LV myocardial TNF- α levels. Whereas in WT mice, plasma TNF- α levels peak at around 2 hours after LPS treatment, *RGS2*^{-/-} mice had increasing TNF- α levels at 4 hours. *RGS2*^{-/-} mice had lower cardiac function than WT at baseline, and RGS2 deficiency further exacerbated cardiac dysfunction during endotoxemia. Our results suggest that p38 is a proinflammatory mediator that is regulated by RGS2 during endotoxemia. (Figure 4.1). While further studies need to be conducted to investigate the specific signaling mechanism through which RGS2 regulates proinflammatory cytokine expression, our study suggests a cardioprotective role of RGS2 in inhibiting proinflammatory signaling in sepsis. The present study suggests a novel therapeutic target for clinical treatment of sepsis. While targeting RGS2 may be complicated due to its central role in many biochemical pathways, this study illuminates possible secondary effects of current clinical drugs, such as the cardiotonic drug digoxin, which upregulates RGS2 activity.¹⁵⁷ This study advances the understanding of sepsis pathogenesis and provides a new therapeutic strategy to combat the high global mortality rate of sepsis.

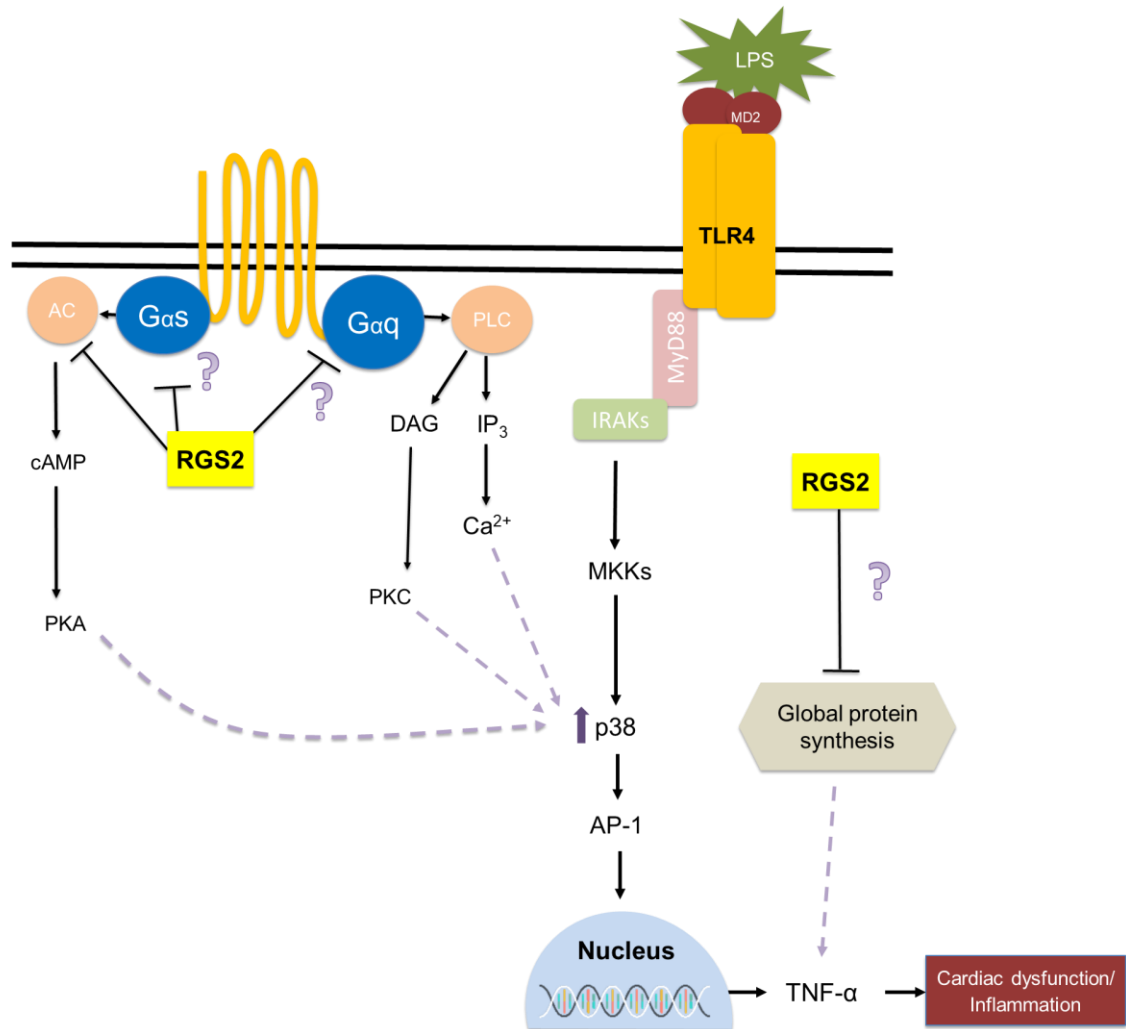


Figure 4.1: Schematic of RGS2 regulation of TNF- α expression during endotoxemia in the heart. TLR4 is activated by LPS, resulting in downstream phosphorylation of p38 MAPK which mediates the production of TNF- α . The induced p38 activity may be inhibited by RGS2 activity, which suppresses possible upstream proinflammatory mediators including PKA, PKC, and Ca²⁺ (indicated by purple dashed arrows). Purple question marks indicate future experiments to investigate the involvement of each distinct RGS2 function (*i.e.* whether RGS2 regulates proinflammatory cytokine production mainly via G α s, G α q, or eIF2B-regulated protein synthesis mechanism).

References

1. Singer, M. *et al.* The third international consensus definitions for sepsis and septic shock (Sepsis-3). *JAMA* **315**, 801 (2016).
2. Martin, G. S., Mannino, D. M. & Moss, M. The effect of age on the development and outcome of adult sepsis. *Crit. Care Med.* **34**, 15–21 (2006).
3. Martin, G. S. & Moss, M. The epidemiology of sepsis in the United States from 1979 through 2000. *N. Engl. J. Med.* **384**, 1546–1554 (2003).
4. Rudd, K. E. *et al.* Global, regional, and national sepsis incidence and mortality, 1990–2017: analysis for the global burden of disease study. *Lancet* **395**, 200–211 (2020).
5. Husak, L. *et al.* National analysis of sepsis hospitalizations and factors contributing to sepsis in-hospital mortality in Canada. *Healthc. Q.* **13**, 35–41 (2010).
6. Winters, B. D. *et al.* Long-term mortality and quality of life in sepsis: a systematic review. *Crit. Care Med.* **38**, 1276–1283 (2010).
7. Yende, S. & Angus, D. C. Long-term outcomes from sepsis. *Curr. Infect. Dis. Rep.* **9**, 382–386 (2007).
8. Iwashyna, T. J., Ely, E. W., Smith, D. M. & Langa, K. M. Long-term cognitive impairment and functional disability among survivors of severe sepsis. *JAMA* **304**, 1787–1794 (2012).
9. Thompson, G. & Kisson, N. Sepsis in Canadian children: a national analysis using administrative data. *Clin. Epidemiol.* **6**, 461–469 (2014).
10. Vincent, J.-L., Jones, G., David, S., Olariu, E. & Cadwell, K. K. Frequency and mortality of septic shock in Europe and North America: a systematic review and meta-analysis. *Crit. Care* **23**, 196 (2019).

11. Andersen, L. W. *et al.* Etiology and therapeutic approach to elevated lactate. *Mayo Clin. Proc.* **88**, 1127–1140 (2013).
12. Scheeren, T. W. L. *et al.* Current use of vasopressors in septic shock. *Ann. Intensive Care* **9**, 20 (2019).
13. Boomer, J. S., Green, J. M. & Hotchkiss, R. S. Is individualized immunomodulatory therapy the answer? *Virulence* **5**, 45–56 (2014).
14. Angus, D. C. & van der Poll, T. Severe sepsis and septic shock. *N. Engl. J. Med.* **369**, 840–851 (2013).
15. Dellinger, R. P. *et al.* Surviving sepsis campaign: international guidelines for management of severe sepsis and septic shock: 2012. *Crit. Care Med.* **315**, 3525–3525 (2017).
16. Pavon, A. *et al.* Profile of the risk of death after septic shock in the present era: an epidemiologic study. *Crit. Care Med.* **41**, 2600–2609 (2013).
17. Marshall, J. C. Why have clinical trials in sepsis failed? *Trends Mol. Med.* **20**, 195–203 (2014).
18. Cohen, J. The immunopathogenesis of sepsis. **420**, 885–891 (2002).
19. Monick, M. M. & Hunninghake, G. W. Second messenger pathways in pulmonary host defense. *Annu. Rev. Physiol.* **65**, 643–667 (2003).
20. Lewis, A. J., Seymour, C. W. & Rosengart, M. R. Current murine models of sepsis. *Surg. Infect.* **17**, 385–393 (2016).
21. Chioléro, R. L. *et al.* Effects of cardiogenic shock on lactate and glucose metabolism after heart surgery. *Crit. Care Med.* **28**, 3784–3791 (2000).
22. Formica, F. *et al.* Extracorporeal membrane oxygenation to support adult patients with cardiac failure: predictive factors of 30-day mortality. *Interact. Cardiovasc. Thorac. Surg.* **10**, 721–726 (2010).

23. Blanco, J. *et al.* Incidence, organ dysfunction and mortality in severe sepsis: A Spanish multicentre study. *Crit. Care* **12**, 1–14 (2008).
24. Fernandes, C. J., Akamine, N. & Knobel, E. Cardiac troponin: A new serum marker of myocardial injury in sepsis. *Intensive Care Med.* **25**, 1165–1168 (1999).
25. Natanson, C. Endotoxin and tumor necrosis factor challenges in dogs simulate the cardiovascular profile of human septic shock. *J. Exp. Med.* **169**, 823–832 (1989).
26. Romero-Bermejo, F. J., Ruiz-Bailen, M., Gil-Cebrian, J. & Huertos-Ranchal, M. J. Sepsis-induced cardiomyopathy. *Curr. Cardiol. Rev.* **7**, 163–183 (2011).
27. Kakihana, Y., Ito, T., Nakahara, M., Yamaguchi, K. & Yasuda, T. Sepsis-induced myocardial dysfunction: pathophysiology and management. *J. Intensive Care* **4**, 22 (2016).
28. MacLean, L. D., Mulligan, W. G., McLean, A. P. & Duff, J. H. Patterns of septic shock in man - a detailed study of 56 patients. *Ann. Surg.* **166**, 543–562 (1967).
29. Parrillo, J. E. *et al.* A circulating myocardial depressant substance in humans with septic shock. *J. Clin. Invest.* **76**, 1539–1553 (1985).
30. Drosatos, K. *et al.* Pathophysiology of sepsis-related cardiac dysfunction: driven by inflammation, energy mismanagement, or both? *Curr. Heart Fail. Rep.* **12**, 130–140 (2015).
31. Fallach, R. *et al.* Cardiomyocyte Toll-like receptor 4 is involved in heart dysfunction following septic shock or myocardial ischemia. *J. Mol. Cell. Cardiol.* **48**, 1236–1244 (2010).
32. Tracey, K. J. *et al.* Shock and tissue injury induced by recombinant human cachectin. *Science* **234**, 470–474 (1986).

33. Peng, T., Lu, X., Lei, M., Moe, G. W. & Feng, Q. Inhibition of p38 MAPK decreases myocardial TNF-alpha expression and improves myocardial function and survival in endotoxemia. *Cardiovasc. Res.* **59**, 893–900 (2003).
34. Grandel, U. *et al.* Endotoxin-induced myocardial tumor necrosis factor-alpha synthesis depresses contractility of isolated rat hearts: evidence for a role of sphingosine and cyclooxygenase-2-derived thromboxane production. *Circulation* **102**, 2758–2764 (2000).
35. Prabhu, S. D. Cytokine-induced modulation of cardiac function. *Circ. Res.* **95**, 1140–1153 (2004).
36. Zhou, P. & Pu, W. T. Recounting cardiac cellular composition. *Circ. Res.* **118**, 368–370 (2016).
37. Yücel, G. *et al.* Lipopolysaccharides induced inflammatory responses and electrophysiological dysfunctions in human-induced pluripotent stem cell derived cardiomyocytes. *Sci. Rep.* **7**, 1–13 (2017).
38. Lackner, I. *et al.* Toll-like receptor-mediated cardiac injury during experimental sepsis. *Mediators Inflamm.* **2020:6051983**, 1–12 (2020).
39. Ammann, P., Fehr, T., Minder, E., Günter, C. & Bertel, O. Elevation of troponin I in sepsis and septic shock. *Intensive Care Med.* **27**, 965–969 (2001).
40. Hamilton, M. A., Toner, A. & Cecconi, M. Troponin in critically ill patients. *Minerva Anesthesiol.* **78**, 1039–1045 (2012).
41. Altmann, D. R. *et al.* Elevated cardiac troponin I in sepsis and septic shock: no evidence for thrombus associated myocardial necrosis. *PLoS ONE* **5**, e9017 (2010).
42. Akira, S. & Takeda, K. Focus of TLR signalling. *Nat. Rev. Immunol.* **4**, 490–511 (2004).

43. Kobe, B. & Kajava, A. V. The leucine-rich repeat as a protein recognition motif. *Curr. Opin. Struct. Biol.* **11**, 725–732 (2001).
44. Van Amersfoort, E. S., Van Berkel, T. J. C. & Kuiper, J. Receptors, mediators, and mechanisms involved in bacterial sepsis and septic shock. *Clin. Microbiol. Rev.* **16**, 379–414 (2003).
45. Raetz, C. R. H. & Whitfield, C. Lipopolysaccharide endotoxins. *Annu. Rev. Biochem.* **71**, 635–700 (2002).
46. Boyd, J., Mathur, S., Wang, Y., Bateman, R. & Walley, K. Toll-like receptor stimulation in cardiomyocytes decreases contractility and initiates an NF- κ B dependent inflammatory response. *Cardiovasc. Res.* **72**, 384–393 (2006).
47. Dauphinee, S. M. & Karsan, A. Lipopolysaccharide signaling in endothelial cells. *Lab. Invest.* **86**, 9–22 (2006).
48. Vaure, C. & Liu, Y. A comparative review of toll-like receptor 4 expression and functionality in different animal species. *Front. Immunol.* **5**, 1–15 (2014).
49. Kuzmich, N. N. *et al.* TLR4 signaling pathway modulators as potential therapeutics in inflammation and sepsis. *Vaccines* **5**, (2017).
50. Guven-Maiorov, E. *et al.* The architecture of the TIR domain signalosome in the toll-like receptor-4 signaling pathway. *Sci. Rep.* **5**, 13128 (2015).
51. Lu, Y.-C., Yeh, W.-C. & Ohashi, P. S. LPS/TLR4 signal transduction pathway. *Cytokine* **42**, 145–151 (2008).
52. Kawai, T. & Akira, S. The roles of TLRs, RLRs and NLRs in pathogen recognition. *Int. Immunol.* **21**, 317–337 (2009).
53. Tang, J. Role of TLR4 in Sepsis. in *Severe Trauma and Sepsis: Organ Damage and Tissue Repair* (eds. Fu, X. & Liu, L.) 113–129 (Springer, 2019). doi:10.1007/978-981-13-3353-8_7.

54. Soriano, F. G., Lorigados, C. B., Pacher, P. & Szabó, C. Effects of a potent peroxynitrite decomposition catalyst in murine models of endotoxemia and sepsis. *Shock* **35**, 560–566 (2011).
55. Ono, Y. *et al.* TAK-242, a specific inhibitor of toll-like receptor 4 signalling, prevents endotoxemia-induced skeletal muscle wasting in mice. *Sci. Rep.* **10**, 694 (2020).
56. Jang, J. C. *et al.* Human resistin protects against endotoxic shock by blocking LPS–TLR4 interaction. *Proc. Natl. Acad. Sci.* **114**, E10399–E10408 (2017).
57. Stan, R. C., Soriano, F. G. & de Camargo, M. M. A mathematical model relates intracellular TLR4 oscillations to sepsis progression. *BMC Res. Notes* **11**, 462 (2018).
58. Wang, Y. *et al.* β 1-adrenoceptor stimulation promotes LPS-induced cardiomyocyte apoptosis through activating PKA and enhancing CaMKII and I κ B α phosphorylation. *Crit. Care* **19**, 76 (2015).
59. Chang, L. & Karin, M. Mammalian MAP kinase signalling cascades. *Nature* **410**, 37–40 (2001).
60. Liu, Y., Shepherd, E. G. & Nelin, L. D. MAPK phosphatases - Regulating the immune response. *Nat. Rev. Immunol.* **7**, 202–212 (2007).
61. Peng, T., Zhang, T., Lu, X. & Feng, Q. JNK1/c-fos inhibits cardiomyocyte TNF- α expression via a negative crosstalk with ERK and p38 MAPK in endotoxaemia. *Cardiovasc. Res.* **81**, 733–741 (2009).
62. Ghil, S., McCoy, K. L. & Hepler, J. R. Regulator of G protein signaling 2 (RGS2) and RGS4 form distinct G protein-dependent complexes with protease activated-receptor 1 (PAR1) in live cells. *PLoS ONE* **9**, 1–9 (2014).
63. Fattahi, F. *et al.* Complement-induced activation of MAPKs and Akt during sepsis: role in cardiac dysfunction. *FASEB J.* **31**, 4129–4139 (2017).

64. Peng, T., Lu, X., Lei, M. & Feng, Q. Endothelial nitric-oxide synthase enhances lipopolysaccharide-stimulated tumor necrosis factor- α expression via cAMP-mediated p38 MAPK pathway in cardiomyocytes. *J. Biol. Chem.* **278**, 8099–8105 (2003).
65. Peng, T., Lu, X. & Feng, Q. Pivotal role of gp91phox-containing NADH oxidase in lipopolysaccharide-induced tumor necrosis factor- α expression and myocardial depression. *Circulation* **111**, 1637–1644 (2005).
66. Brereton, C. F., Sutton, C. E., Lalor, S. J., Lavelle, E. C. & Mills, K. H. G. Inhibition of ERK MAPK suppresses IL-23- and IL-1-driven IL-17 production and attenuates autoimmune disease. *J. Immunol.* **183**, 1715–1723 (2009).
67. Han, J., Lee, J., Bibbs, L. & Ulevitch, R. A MAP kinase targeted by endotoxin and hyperosmolarity in mammalian cells. *Science* **265**, 808–811 (1994).
68. Zhang, J., Shen, B. & Lin, A. Novel strategies for inhibition of the p38 MAPK pathway. *Trends Pharmacol. Sci.* **28**, 286–295 (2007).
69. Wang, J., Tang, R., Lv, M., Zhang, J. & Shen, B. Selective unresponsiveness to the inhibition of p38 MAPK activation by cAMP helps L929 fibroblastoma cells escape TNF- α -induced cell death. *Mol. Cancer* **9**, 6 (2010).
70. Goldsmith, Z. G. & Dhanasekaran, D. N. G Protein regulation of MAPK networks. *Oncogene* **26**, 3122–3142 (2007).
71. Zhang, T. *et al.* Mitogen-activated protein kinase phosphatase-1 inhibits myocardial TNF- α expression and improves cardiac function during endotoxemia. *Cardiovasc. Res.* **93**, 471–479 (2012).
72. Zhang, J. *et al.* Cyclic AMP inhibits JNK activation by CREB-mediated induction of c-FLIPL and MKP-1, thereby antagonizing UV-induced apoptosis. *Cell Death Differ.* **15**, 1654–1662 (2008).

73. Roy, P. K., Rashid, F., Bragg, J. & Ibdah, J. A. Role of the JNK signal transduction pathway in inflammatory bowel disease. *World J. Gastroenterol. WJG* **14**, 200–202 (2008).
74. Zhang, Q., Lenardo, M. J. & Baltimore, D. 30 years of NF- κ B: a blossoming of relevance to human pathobiology. *Cell* **168**, 37–57 (2017).
75. Kawai, T. & Akira, S. Signaling to NF- κ B by toll-like receptors. *Trends Mol. Med.* **13**, 460–469 (2007).
76. Karin, M. & Delhase, M. The I kappa B kinase (IKK) and NF-kappa B: key elements of proinflammatory signalling. *Semin. Immunol.* **12**, 85–98 (2000).
77. Liu, T., Zhang, L., Joo, D. & Sun, S.-C. NF- κ B signaling in inflammation. *Signal Transduct. Target. Ther.* **2**, 17023 (2017).
78. Israël, A. The IKK complex, a central regulator of NF-kappaB activation. *Cold Spring Harb. Perspect. Biol.* **2**, a000158 (2010).
79. Kawai, T., Adachi, O., Ogawa, T., Takeda, K. & Akira, S. Unresponsiveness of MyD88-deficient mice to endotoxin. *Immunity* **11**, 115–122 (1999).
80. Shim, J.-H. *et al.* TAK1, but not TAB1 or TAB2, plays an essential role in multiple signaling pathways in vivo. *Genes Dev.* **19**, 2668–2681 (2005).
81. Yamamoto, M. *et al.* Role of adaptor TRIF in the MyD88-independent toll-like receptor signaling pathway. *Science* **301**, 640–643 (2003).
82. Perez, J. M., Chirieleison, S. M. & Abbott, D. W. An I κ B Kinase-regulated feed-forward circuit prolongs inflammation. *Cell Rep.* **12**, 537–544 (2015).
83. Neves, S., Ram, P. & Iyengar, R. G Protein pathways. *Science* **296**, 1636–1640 (2002).

84. Chidiac, P. RGS proteins destroy spare receptors: Effects of GPCR-interacting proteins and signal deamplification on measurements of GPCR agonist potency. *Methods* **92**, 87–93 (2016).
85. Hendriks-balk, M. C., Peters, S. L. M., Michel, M. C. & Alewijnse, A. E. Regulation of G protein-coupled receptor signalling : Focus on the cardiovascular system and regulator of G protein signalling proteins. *Eur. J. Pharmacol.* **585**, 278–291 (2008).
86. Oldham, W. M. & Hamm, H. E. Heterotrimeric G protein activation by G-protein-coupled receptors. *Nat. Rev. Mol. Cell Biol.* **9**, 60–71 (2008).
87. Akimoto, M., VanSchouwen, B. & Melacini, G. The structure of the apo cAMP-binding domain of HCN4 – a stepping stone toward understanding the cAMP-dependent modulation of the hyperpolarization-activated cyclic-nucleotide-gated ion channels. *FEBS J.* **285**, 2182–2192 (2018).
88. Pierce, K. L., Premont, R. T. & Lefkowitz, R. J. Seven-transmembrane receptors. *Nat. Rev. Mol. Cell Biol.* **3**, 639–650 (2002).
89. Lutz, S. *et al.* Structure of Galphaq-p63RhoGEF-RhoA complex reveals a pathway for the activation of RhoA by GPCRs. *Science* **318**, 1923–1927 (2007).
90. Bos, J. L. Epac proteins: multi-purpose cAMP targets. *Trends Biochem. Sci.* **31**, 680–686 (2006).
91. Laroche-Joubert, N., Marsy, S., Michelet, S., Imbert-Teboul, M. & Doucet, A. Protein kinase A-independent activation of ERK and H,K-ATPase by cAMP in native kidney cells: role of Epac I. *J. Biol. Chem.* **277**, 18598–18604 (2002).
92. Enserink, J. M. *et al.* A novel Epac-specific cAMP analogue demonstrates independent regulation of Rap1 and ERK. *Nat. Cell Biol.* **4**, 901–906 (2002).
93. Graves, L. M. *et al.* Protein kinase A antagonizes platelet-derived growth factor-induced signaling by mitogen-activated protein kinase in human arterial smooth muscle cells. *Proc. Natl. Acad. Sci. U. S. A.* **90**, 10300–10304 (1993).

94. Norum, J. H., Méthi, T., Mattingly, R. R. & Levy, F. O. Endogenous expression and protein kinase A-dependent phosphorylation of the guanine nucleotide exchange factor Ras-GRF1 in human embryonic kidney 293 cells. *FEBS J.* **272**, 2304–2316 (2005).
95. Yang, L. *et al.* Loss of β -adrenergic-stimulated phosphorylation of CaV1.2 channels on Ser1700 leads to heart failure. *Proc. Natl. Acad. Sci.* **113**, E7976–E7985 (2016).
96. Zheng, M. *et al.* beta 2-adrenergic receptor-induced p38 MAPK activation is mediated by protein kinase A rather than by Gi or gbeta gamma in adult mouse cardiomyocytes. *J. Biol. Chem.* **275**, 40635–40640 (2000).
97. Edamatsu, H., Kaziro, Y. & Itoh, H. Expression of an oncogenic mutant G alpha i2 activates Ras in Rat-1 fibroblast cells. *FEBS Lett.* **440**, 231–234 (1998).
98. Pace, A. M., Faure, M. & Bourne, H. R. Gi2-mediated activation of the MAP kinase cascade. *Mol. Biol. Cell* **6**, 1685–1695 (1995).
99. Blaukat, A., Barac, A., Cross, M. J., Offermanns, S. & Dikic, I. G protein-coupled receptor-mediated mitogen-activated protein kinase activation through cooperation of Galpha(q) and Galpha(i) signals. *Mol. Cell. Biol.* **20**, 6837–6848 (2000).
100. Guo, F. F., Kumahara, E. & Saffen, D. A CalDAG-GEFI/Rap1/B-Raf cassette couples M(1) muscarinic acetylcholine receptors to the activation of ERK1/2. *J. Biol. Chem.* **276**, 25568–25581 (2001).
101. Huang, C.-C., You, J.-L., Wu, M.-Y. & Hsu, K.-S. Rap1-induced p38 mitogen-activated protein kinase activation facilitates AMPA receptor trafficking via the GDI.Rab5 complex. Potential role in (S)-3,5-dihydroxyphenylglycine-induced long term depression. *J. Biol. Chem.* **279**, 12286–12292 (2004).
102. Wang, J., Gareri, C. & Rockman, H. A. G protein-coupled receptors in heart disease. *Circ. Res.* **123**, 716–735 (2018).

103. Tariq, S. & Aronow, W. S. Use of inotropic agents in treatment of systolic heart failure. *Int. J. Mol. Sci.* **16**, 29060–29068 (2015).
104. Annane, D. *et al.* Inappropriate sympathetic activation at onset of septic shock: a spectral analysis approach. *Am. J. Respir. Crit. Care Med.* **160**, 458–465 (1999).
105. Dünser, M. W. & Hasibeder, W. R. Sympathetic overstimulation during critical illness: adverse effects of adrenergic stress. *J. Intensive Care Med.* **24**, 293–316 (2009).
106. Galaz-Montoya, M., Wright, S. J., Rodriguez, G. J., Lichtarge, O. & Wensel, T. G. β 2-Adrenergic receptor activation mobilizes intracellular calcium via a non-canonical cAMP-independent signaling pathway. *J. Biol. Chem.* **292**, 9967–9974 (2017).
107. Gulick, T., Chung, M. K., Pieper, S. J., Lange, L. G. & Schreiner, G. F. Interleukin 1 and tumor necrosis factor inhibit cardiac myocyte beta-adrenergic responsiveness. *Proc. Natl. Acad. Sci. U. S. A.* **86**, 6753–6757 (1989).
108. Jensen, B. C., O’Connell, T. D. & Simpson, P. C. Alpha-1-Adrenergic Receptors in Heart Failure: The Adaptive Arm of the Cardiac Response to Chronic Catecholamine Stimulation. *J. Cardiovasc. Pharmacol.* **63**, 291–301 (2014).
109. Jensen, B. C., Swigart, P. M., De Marco, T., Hoopes, C. & Simpson, P. C. {alpha}1-Adrenergic receptor subtypes in nonfailing and failing human myocardium. *Circ. Heart Fail.* **2**, 654–663 (2009).
110. Bristow, M. R. *et al.* Decreased catecholamine sensitivity and beta-adrenergic-receptor density in failing human hearts. *N. Engl. J. Med.* **307**, 205–211 (1982).
111. Wu, L.-L. *et al.* G protein and adenylate cyclase complex-mediated signal transduction in the rat heart during sepsis. *Shock* **19**, 533–537 (2003).
112. Risøe, P. K. *et al.* Lipopolysaccharide attenuates mRNA levels of several adenylyl cyclase isoforms in vivo. *Biochim. Biophys. Acta* **1772**, 32–39 (2007).

113. Sakai, M. *et al.* Diminished responsiveness to dobutamine as an inotrope in mice with cecal ligation and puncture-induced sepsis: attribution to phosphodiesterase 4 upregulation. *Am. J. Physiol. Heart Circ. Physiol.* **312**, H1224–H1237 (2017).
114. Bucher, M., Kees, F., Taeger, K. & Kurtz, A. Cytokines down-regulate α 1-adrenergic receptor expression during endotoxemia. *Crit. Care Med.* **31**, 566–571 (2003).
115. Nevieri, R. *et al.* Abnormal mitochondrial cAMP/PKA signaling is involved in sepsis-induced mitochondrial and myocardial dysfunction. *Int. J. Mol. Sci.* **17**, 2075 (2016).
116. Mitra, S. & Bourreau, J. P. Gs and Gi coupling of adrenomedullin in adult rat ventricular myocytes. *Am. J. Physiol. - Heart Circ. Physiol.* **290**, 1842–1847 (2006).
117. Elenkov, I. J., Haskó, G., Kovács, K. J. & Vizi, E. S. Modulation of lipopolysaccharide-induced tumor necrosis factor- α production by selective alpha- and beta-adrenergic drugs in mice. *J. Neuroimmunol.* **61**, 123–131 (1995).
118. Miksa, M. *et al.* Pivotal role of the α 2A-adrenoceptor in producing inflammation and organ injury in a rat model of sepsis. *PLOS ONE* **4**, e5504 (2009).
119. Qiu, R. *et al.* Dexmedetomidine restores septic renal function via promoting inflammation resolution in a rat sepsis model. *Life Sci.* **204**, 1–8 (2018).
120. Kaur, M. & Singh, P. M. Current role of dexmedetomidine in clinical anesthesia and intensive care. *Anesth. Essays Res.* **5**, 128–133 (2011).
121. Ross, E. M. & Wilkie, T. M. GTPase-activating proteins for heterotrimeric G proteins: regulators of G protein signaling (RGS) and RGS-like proteins. *Annu. Rev. Biochem.* **69**, 795–827 (2000).
122. Popov, S., Yu, K., Kozasa, T. & Wilkie, T. M. The regulators of G protein signaling (RGS) domains of RGS4, RGS10, and GAIP retain GTPase activating protein activity in vitro. *Proc. Natl. Acad. Sci.* **94**, 7216–7220 (1997).

123. Roy, A. A. *et al.* RGS2 interacts with Gs and adenylyl cyclase in living cells. *Cell. Signal.* **18**, 336–348 (2006).
124. Abramow-Newerly, M., Roy, A. A., Nunn, C. & Chidiac, P. RGS proteins have a signalling complex: Interactions between RGS proteins and GPCRs, effectors, and auxiliary proteins. *Cell. Signal.* **18**, 579–591 (2006).
125. Melliti, K., Meza, U. & Adams, B. Muscarinic stimulation of alpha1E Ca channels is selectively blocked by the effector antagonist function of RGS2 and phospholipase C-beta1. *J. Neurosci. Off. J. Soc. Neurosci.* **20**, 7167–7173 (2000).
126. Anger, T., Zhang, W. & Mende, U. Differential contribution of GTPase activation and effector antagonism to the inhibitory effect of RGS proteins on Gq-mediated signaling in vivo. *J. Biol. Chem.* **279**, 3906–3915 (2004).
127. Mittmann, C. *et al.* Expression of ten RGS proteins in human myocardium: functional characterization of an upregulation of RGS4 in heart failure. *Cardiovasc. Res.* **55**, 778–786 (2002).
128. Rorabaugh, B. R. *et al.* Regulator of G protein signaling 6 protects the heart from ischemic injury. *J. Pharmacol. Exp. Ther.* **360**, 409–416 (2016).
129. Doupnik, C. A., Xu, T. & Shinaman, J. M. Profile of RGS expression in single rat atrial myocytes. *Biochim. Biophys. Acta BBA - Gene Struct. Expr.* **1522**, 97–107 (2001).
130. Riddle Evan L., Schwartzman Raúl A., Bond Meredith & Insel Paul A. Multi-tasking RGS proteins in the heart. *Circ. Res.* **96**, 401–411 (2005).
131. Zhang, P. *et al.* Regulator of G protein signaling 2 is a functionally important negative regulator of angiotensin II-induced cardiac fibroblast responses. *Am. J. Physiol. - Heart Circ. Physiol.* **301**, H147–H156 (2011).
132. Takiuchi, S. *et al.* Genetic variations of regulator of G-protein signaling 2 in hypertensive patients and in the general population. *J. Hypertens.* **23**, 1497–1505 (2005).

133. Gu, S., Cifelli, C., Wang, S. & Heximer, S. P. RGS proteins: identifying new GAPs in the understanding of blood pressure regulation and cardiovascular function. *Clin. Sci.* **116**, 391–399 (2009).
134. Sjögren, B. & Neubig, R. R. Thinking outside of the “RGS Box”: New approaches to therapeutic targeting of regulators of G protein signaling. *Mol. Pharmacol.* **78**, 550–557 (2010).
135. Zhang, W. *et al.* Selective loss of fine tuning of Gq/11 signaling by RGS2 protein exacerbates cardiomyocyte hypertrophy. *J. Biol. Chem.* **281**, 5811–5820 (2006).
136. Tang, M. *et al.* Regulator of G-protein signaling-2 mediates vascular smooth muscle relaxation and blood pressure. *Nat. Med.* **9**, 1506–1512 (2003).
137. Mittmann, C. *et al.* Expression of ten RGS proteins in human myocardium: functional characterization of an upregulation of RGS4 in heart failure. *Cardiovasc. Res.* **55**, 778–786 (2002).
138. Roy, A. A., Lemberg, K. E. & Chidiac, P. Recruitment of RGS2 and RGS4 to the plasma membrane by G proteins and receptors reflects functional interactions. *Mol. Pharmacol.* **64**, 587–593 (2003).
139. Bernstein, L. S. *et al.* RGS2 binds directly and selectively to the M1 muscarinic acetylcholine receptor third intracellular loop to modulate Gq/11 α signaling. *J. Biol. Chem.* **279**, 21248–21256 (2004).
140. Hague, C. *et al.* Selective inhibition of α 1A-adrenergic receptor signaling by RGS2 association with the receptor third intracellular loop. *J. Biol. Chem.* **280**, 27289–27295 (2005).
141. Wang, C.-H. (Jenny) & Chidiac, P. RGS2 promotes the translation of stress-associated proteins ATF4 and CHOP via its eIF2B-inhibitory domain. *Cell. Signal.* **59**, 163–170 (2019).

142. Nguyen, C. H. *et al.* Translational control by RGS2. *J. Cell Biol.* **186**, 755–765 (2009).
143. Cunningham, M. L., Waldo, G. L., Hollinger, S., Hepler, J. R. & Harden, T. K. Protein kinase C phosphorylates RGS2 and modulates its capacity for negative regulation of Gα11 signaling. *J. Biol. Chem.* **276**, 5438–5444 (2001).
144. Osei-Owusu, P., Sun, X., Drenan, R. M., Steinberg, T. H. & Blumer, K. J. Regulation of RGS2 and second messenger signaling in vascular smooth muscle cells by cGMP-dependent protein kinase. *J. Biol. Chem.* **282**, 31656–31665 (2007).
145. Kanai, S. M., Edwards, A. J., Rurik, J. G., Osei-Owusu, P. & Blumer, K. J. Proteolytic degradation of regulator of G protein signaling 2 facilitates temporal regulation of Gq/11 signaling and vascular contraction. *J. Biol. Chem.* **292**, 19266–19278 (2017).
146. Davis, M. J. & Hill, M. A. Signaling mechanisms underlying the vascular myogenic response. *Physiol. Rev.* **79**, 387–423 (1999).
147. Offermanns, S. G-proteins as transducers in transmembrane signalling. *Prog. Biophys. Mol. Biol.* **83**, 101–130 (2003).
148. Wettschureck, N. *et al.* Absence of pressure overload induced myocardial hypertrophy after conditional inactivation of Gα11 in cardiomyocytes. *Nat. Med.* **7**, 1236–1240 (2001).
149. Heximer, S. P. *et al.* Hypertension and prolonged vasoconstrictor signaling in RGS2-deficient mice. *J. Clin. Invest.* **111**, 445–452 (2003).
150. Tuomi, J. M., Chidiac, P. & Jones, D. L. Evidence for enhanced M3 muscarinic receptor function and sensitivity to atrial arrhythmia in the RGS2-deficient mouse. *Am. J. Physiol.-Heart Circ. Physiol.* **298**, H554–H561 (2010).
151. Jones, D. L., Tuomi, J. M. & Chidiac, P. Role of cholinergic innervation and RGS2 in atrial arrhythmia. *Front. Physiol.* **3**, 1–12 (2012).

152. Takimoto, E. *et al.* Regulator of G protein signaling 2 mediates cardiac compensation to pressure overload and antihypertrophic effects of PDE5 inhibition in mice. *J. Clin. Invest.* **119**, 408–420 (2009).
153. Pessina, A. C. *et al.* Reduced expression of regulator of G-protein signaling 2 (RGS2) in hypertensive patients increases calcium mobilization and ERK1/2 phosphorylation induced by angiotensin II. *J. Hypertens.* **24**, 1115–1124 (2006).
154. Calò, L. A. *et al.* Increased expression of regulator of G protein signaling-2 (RGS-2) in Bartter's/Gitelman's syndrome. A role in the control of vascular tone and implication for hypertension. *J. Clin. Endocrinol. Metab.* **89**, 4153–4157 (2004).
155. Zou, M.-X. *et al.* RGS2 is upregulated by and attenuates the hypertrophic effect of alpha1-adrenergic activation in cultured ventricular myocytes. *Cell. Signal.* **18**, 1655–1663 (2006).
156. Nunn, C. *et al.* RGS2 inhibits β -adrenergic receptor-induced cardiomyocyte hypertrophy. *Cell. Signal.* **22**, 1231–1239 (2010).
157. Sjögren, B., Parra, S., Atkins, K. B., Karaj, B. & Neubig, R. R. Digoxin-mediated upregulation of RGS2 protein protects against cardiac injury. *J. Pharmacol. Exp. Ther.* **357**, 311–319 (2016).
158. Semplicini, A. *et al.* Reduced expression of regulator of G-protein signaling 2 (RGS2) in hypertensive patients increases calcium mobilization and ERK1/2 phosphorylation induced by angiotensin II. *J. Hypertens.* **24**, 1115–1124 (2006).
159. Zhang, S. & Lin, X. CARMA3: Scaffold protein involved in NF- κ B signaling. *Front. Immunol.* **10**, 176 (2019).
160. Zhang, T. *et al.* Inhibition of Na/K-ATPase promotes myocardial tumor necrosis factor-alpha protein expression and cardiac dysfunction via calcium/mTOR signaling in endotoxemia. *Basic Res. Cardiol.* **107**, 254 (2012).

161. Lee, K. N., Lu, X., Nguyen, C., Feng, Q. & Chidiac, P. Cardiomyocyte specific overexpression of a 37 amino acid domain of regulator of G protein signalling 2 inhibits cardiac hypertrophy and improves function in response to pressure overload in mice. *J. Mol. Cell. Cardiol.* **108**, 194–202 (2017).
162. Wishaw, I. Q. *et al.* Regulation of T cell activation, anxiety, and male aggression by RGS2. *Proc. Natl. Acad. Sci.* **97**, 12272–12277 (2002).
163. Roy, A. A. *et al.* Up-regulation of endogenous RGS2 mediates cross-desensitization between Gs and Gq signaling in osteoblasts. *J. Biol. Chem.* **281**, 32684–32693 (2006).
164. Kuo, S.-M. Gender difference in bacteria endotoxin-induced inflammatory and anorexic responses. *PLOS ONE* **11**, e0162971 (2016).
165. Kennedy, L. H., Hwang, H., Wolfe, A. M., Hauptman, J. & Nemzek-Hamlin, J. A. Effects of buprenorphine and estrous cycle in a murine model of cecal ligation and puncture. *Comp. Med.* **64**, 270–282 (2014).
166. Song, W., Lu, X. & Feng, Q. Tumor necrosis factor- α induces apoptosis via inducible nitric oxide synthase in neonatal mouse cardiomyocytes. *Cardiovasc. Res.* **45**, 595–602 (2000).
167. Hammoud, L., Burger, D. E., Lu, X. & Feng, Q. Tissue inhibitor of metalloproteinase-3 inhibits neonatal mouse cardiomyocyte proliferation via EGFR/JNK/SP-1 signaling. *Am. J. Physiol.-Cell Physiol.* **296**, C735–C745 (2009).
168. Nguyen, C. H., Zhao, P., Sobiesiak, A. J. & Chidiac, P. RGS2 is a component of the cellular stress response. *Biochem. Biophys. Res. Commun.* **426**, 129–134 (2012).
169. Nunn, C. *et al.* Resistance to age-related, normal body weight gain in RGS2 deficient mice. *Cell. Signal.* **23**, 1375–1386 (2011).
170. Bernhardt, M. L. *et al.* Regulator of G-protein signaling 2 (RGS2) suppresses premature calcium release in mouse eggs. *Dev. Camb. Engl.* **142**, 2633–2640 (2015).

171. Kach, J., Sethakorn, N. & Dulin, N. O. A finer tuning of G-protein signaling through regulated control of RGS proteins. *Am. J. Physiol.-Heart Circ. Physiol.* **303**, H19–H35 (2012).
172. Hao, J. *et al.* Regulation of cardiomyocyte signaling by RGS proteins: Differential selectivity towards G proteins and susceptibility to regulation. *J. Mol. Cell. Cardiol.* **41**, 51–61 (2006).
173. Copeland, S., Warren, H. S., Lowry, S. F., Calvano, S. E. & Remick, D. Acute inflammatory response to endotoxin in mice and humans. *Clin. Diagn. Lab. Immunol.* **12**, 60–67 (2005).
174. Sassone-Corsi, P. The cyclic AMP pathway. *Cold Spring Harb. Perspect. Biol.* **4**, (2012).
175. Klepac, K., Yang, J., Hildebrand, S. & Pfeifer, A. RGS2: A multifunctional signaling hub that balances brown adipose tissue function and differentiation. *Mol. Metab.* **30**, 173–183 (2019).
176. Cheng, Y.-S., Lee, T.-S., Hsu, H.-C., Kou, Y. R. & Wu, Y.-L. Characterization of the transcriptional regulation of the regulator of G protein signaling 2 (RGS2) gene during 3T3-L1 preadipocyte differentiation. *J. Cell. Biochem.* **105**, 922–930 (2008).
177. George, T., Chakraborty, M., Giembycz, M. A. & Newton, R. A bronchoprotective role for Rgs2 in a murine model of lipopolysaccharide-induced airways inflammation. *Allergy Asthma Clin. Immunol.* **14**, 40 (2018).
178. Panetta, R., Guo, Y., Magder, S. & Greenwood, M. T. Regulators of G-protein signaling (RGS) 1 and 16 are induced in response to bacterial lipopolysaccharide and stimulate c-fos promoter expression. *Biochem. Biophys. Res. Commun.* **259**, 550–556 (1999).
179. Suurväli, J. *et al.* RGS16 restricts the pro-inflammatory response of monocytes. *Scand. J. Immunol.* **81**, 23–30 (2015).

180. Alqinyah, M., Almutairi, F., Wendimu, M. Y. & Hooks, S. B. RGS10 regulates the expression of cyclooxygenase-2 and tumor necrosis factor alpha through a G protein-independent mechanism. *Mol. Pharmacol.* **94**, 1103–1113 (2018).
181. Yang, S. *et al.* Inhibition of Rgs10 expression prevents immune cell infiltration in bacteria-induced inflammatory lesions and osteoclast-mediated bone destruction. *Bone Res.* **1**, 267–281 (2013).
182. Patten, M. *et al.* Endotoxin induces desensitization of cardiac endothelin-1 receptor signaling by increased expression of RGS4 and RGS16. *Cardiovasc. Res.* **53**, 156–164 (2002).
183. Grant, S. L. *et al.* Specific regulation of RGS2 messenger RNA by angiotensin II in cultured vascular smooth muscle cells. *Mol. Pharmacol.* **57**, 460–467 (2000).
184. Riekenberg, S. *et al.* Regulators of G-protein signalling are modulated by bacterial lipopeptides and lipopolysaccharide. *FEBS J.* **276**, 649–659 (2009).
185. Lee, H.-K. *et al.* Protein kinase C- η and phospholipase D2 pathway regulates foam cell formation via regulator of G protein signaling 2. *Mol. Pharmacol.* **78**, 478–485 (2010).
186. Shi, G.-X., Harrison, K., Han, S.-B., Moratz, C. & Kehrl, J. H. Toll-like receptor signaling alters the expression of regulator of G protein signaling proteins in dendritic cells: implications for G protein-coupled receptor signaling. *J. Immunol. Baltim. Md 1950* **172**, 5175–5184 (2004).
187. Zaghoul, N. *et al.* Forebrain cholinergic dysfunction and systemic and brain inflammation in murine sepsis survivors. *Front. Immunol.* **8**, 1673 (2017).
188. Lieb, K. *et al.* Interleukin-1 beta uses common and distinct signaling pathways for induction of the interleukin-6 and tumor necrosis factor alpha genes in the human astrocytoma cell line U373. *J. Neurochem.* **66**, 1496–1503 (1996).

189. Van Linthout, S. & Tschöpe, C. Inflammation – cause or consequence of heart failure or both? *Curr. Heart Fail. Rep.* **14**, 251–265 (2017).
190. Jahng, J. W. S., Song, E. & Sweeney, G. Crosstalk between the heart and peripheral organs in heart failure. *Exp. Mol. Med.* **48**, e217 (2016).
191. Torre-Amione, G. *et al.* Proinflammatory cytokine levels in patients with depressed left ventricular ejection fraction: a report from the Studies of Left Ventricular Dysfunction (SOLVD). *J. Am. Coll. Cardiol.* **27**, 1201–1206 (1996).
192. Hoffman, M. *et al.* Myocardial strain and cardiac output are preferable measurements for cardiac dysfunction and can predict mortality in septic mice. *J. Am. Heart Assoc. Cardiovasc. Cerebrovasc. Dis.* **8**, 1–20 (2019).
193. Smalley, M. J. *et al.* Regulator of G-protein signalling 2 mRNA is differentially expressed in mammary epithelial subpopulations and over-expressed in the majority of breast cancers. *Breast Cancer Res.* **9**, R85 (2007).
194. Ye, R. D. Regulation of nuclear factor κ B activation by G-protein-coupled receptors. *J. Leukoc. Biol.* **70**, 839–848 (2001).

Appendices

Appendix A: Animal use protocol approved by the Animal Care Committee

Qingping Feng

From: [REDACTED]
Sent: Friday, November 1, 2019 12:41 PM
To: Qingping Feng; ACC Office
Subject: eSirius3G Notification -- 2016-099 Annual Renewal Approved



2016-099:12

AUP Number: 2016-099
AUP Title: Modulation of Myocardial Function in Myocardial Infarction, Sepsis and Diabetes
Yearly Renewal Date: 11/01/2020

The YEARLY RENEWAL to Animal Use Protocol (AUP) 2016-099 has been approved by the Animal Care Committee (ACC), and will be approved through to the above review date.

Please at this time review your AUP with your research team to ensure full understanding by everyone listed within this AUP.

As per your declaration within this approved AUP, you are obligated to ensure that:

- 1) Animals used in this research project will be cared for in alignment with:
 - a) Western's Senate MAPPs 7.12, 7.10, and 7.15
http://www.uwo.ca/univsec/policies_procedures/research.html
 - b) University Council on Animal Care Policies and related Animal Care Committee procedures

http://uwo.ca/research/services/animalethics/animal_care_and_use_policies.html

- 2) As per UCAC's Animal Use Protocols Policy,
 - a) this AUP accurately represents intended animal use;
 - b) external approvals associated with this AUP, including permits and scientific/departmental peer approvals, are complete and accurate;
 - c) any divergence from this AUP will not be undertaken until the related Protocol Modification is approved by the ACC; and
 - d) AUP form submissions - Annual Protocol Renewals and Full AUP Renewals - will be submitted and attended to within timeframes outlined by the ACC.

http://uwo.ca/research/services/animalethics/animal_use_protocols.html

- 3) As per MAPP 7.10 all individuals listed within this AUP as having any hands-on animal contact will
 - a) be made familiar with and have direct access to this AUP;
 - b) complete all required CCAC mandatory training [REDACTED]; and
 - c) be overseen by me to ensure appropriate care and use of animals.

- 4) As per MAPP 7.15,
 - a) Practice will align with approved AUP elements;
 - b) Unrestricted access to all animal areas will be given to ACVS Veterinarians

and ACC Leaders;

- limited to:
- c) UCAC policies and related ACC procedures will be followed, including but not
 - i) Research Animal Procurement
 - ii) Animal Care and Use Records

- iii) Sick Animal Response
- iv) Continuing Care Visits

5) As per institutional OH&S policies, all individuals listed within this AUP who will be using or potentially exposed to hazardous materials will have completed in advance the appropriate institutional OH&S training, facility-level training, and reviewed related (M)SDS Sheets, <http://www.uwo.ca/hr/learning/required/index.html>

Submitted by: Copeman, Laura
on behalf of the Animal Care Committee
University Council on Animal Care



Western Ontario
Council on Animal Care
N6A 5C1

The University of
Animal Care Committee / University
London, Ontario Canada

Curriculum Vitae

Name: Xin Tong Carol Ma

Post-secondary Education and Degrees: University of Western Ontario
London, Ontario, Canada
2014-2018 BMSc.

Honours and Awards: The Western Scholarship of Excellence
2014

Dean's Honor List
2014-2018

Western Graduate Research Scholarship
2018-2020

Malcolm Arnold Cardiovascular Sciences Poster Award
2019

Province of Ontario Graduate Scholarship
2019-2020

CSPT Members Choice Presentation Award
2020

Related Work Experience Research Assistant
University of Western Ontario
2016-2017

Teaching Assistant
University of Western Ontario
2019-2020

Presentations:

The Department of Physiology and Pharmacology Research Day, London, ON, 2018.
Title: The Role of Regulator of G protein Signaling 2 in Inflammatory Cytokine Release in Mice with Endotoxemia.

London Health Research Day, London, ON, 2018.
Title: The Role of Regulator of G protein Signaling 2 in Inflammatory Cytokine Release in Endotoxemic Mice.

The Department of Physiology and Pharmacology Research Day, London, ON, 2019.
Title: The Role of Regulator of G protein Signaling 2 in Inflammatory Cytokine Release
in Endotoxemic Mice.

Canadian Society of Pharmacology and Therapeutics Annual Conference, 2020.
Title: The Role of RGS2 in Inflammatory Cytokine Release in Endotoxemia in Mice.